# Tailoring Wing Structures for Reduced Drag Penalty in Off-design Flight Conditions

Melih Papila[1] and Raphael T. Haftka.[2]
*University of Florida, Gainesville, FL, 32611-6250*

William H. Mason[3]
*Virginia Polytechnic Institute and State University, Blacksburg, VA 24061-0203*

*and*

Rafael Alves[4]
*Instituto Tecnologico de Aeronautica, Brasil*

**The induced drag penalty associated with off-design flight conditions is investigated. The investigation is limited to off-design flight conditions at a lower lift coefficient than the design lift coefficient. Two types of total angle of incidence distribution obtained at the design condition are studied. One is the distribution for elliptic spanloads and the other is the spanload distribution for straight-line wrapped surfaces. It is shown that the penalty may be significant as the structural deformation changes the total angle of incidence distribution and the spanload. The penalty is higher for the wing with the near optimal elliptic spanload at the design flight condition. The wing with straight-line wrapped surfaces does not have the minimum induced drag at the design condition. However, it is found to be insensitive to the structural deformation.**

## NOMENCLATURE

| | | |
|---|---|---|
| $^{(1)}$ | = | Design flight condition |
| $^{(2)}$ | = | Off-design flight condition |
| $C_L^{(1)}, C_L^{(2)}$ | = | Lift coefficients at design and off-design flight conditions |
| $h^{(1)}, h^{(2)}$ | = | Flight altitudes of design and off-design flight conditions |
| $W^{(1)}, W^{(2)}$ | = | Cruise weights of design and off-design flight conditions |
| $\alpha(\eta)$ | = | Geometric twist distribution as built into wing |

[1] Post Doctoral Research Associate, Department of Mechanical and Aerospace Engineering, University of Florida, Gainesville, FL 32611-6250, Member AIAA.
[2] Distinguished Professor, Department of Mechanical and Aerospace Engineering, University of Florida, Gainesville, FL 32611-6250, Fellow AIAA.
[3] Professor, Department of Aerospace and Ocean Engineering, Virginia Polytechnic Institute and State University, Blacksburg, VA 24061-0203, Associate Fellow AIAA.
[4] Student, Instituto Tecnologico de Aeronautica, Brasil

$\alpha(\eta)\big|_{rigid}$ = Geometric twist distribution as built into rigid wing,

$\alpha_{opt}^{(1)}(\eta)$ = Optimal geometric twist distribution at design flight condition

$\alpha_{opt}^{(2)}(\eta)$ = Optimal geometric twist distribution at off-design flight condition

$\alpha_{non}^{(2)}(\eta)$ = Non-optimal geometric twist distribution at the off-design condition

$\overline{\alpha}^{(1)}, \overline{\alpha}^{(2)}$ = Angle of attack for design and off-design conditions

$\alpha_{def}(\alpha(\eta), \overline{\alpha})$ = Deformation twist associated with structural deformation for given geometric twist $\alpha(\eta)$ and angle of attack $\overline{\alpha}$

$\alpha_{elas}(\eta)$ = Elastic wing twist, sum of the geometric twist and deformation twist

$\alpha_{tot}(\eta)$ =: Total angle of incidence distribution, sum of elastic twist and the angle of attack

$w_{LE}(\eta)$ = Lateral displacement at the leading edge

$w_{TE}(\eta)$ = Lateral displacement at the trailing edge

## I. INTRODUCTION

The wing of an airplane as built is in general not optimal at all flight conditions. As far as wing twist is concerned, different optimal geometric twists are associated with different flight conditions, as Lynch and Rogers[1] (1976) reported for a bomber wing. They stated the wing twist at cruise (1g load factor) was not optimal for a maneuver at a higher load factor, 7.33g. Haftka[2] (1977) showed that aeroelastic tailoring can be used in composite wings to reduce the drag penalty at very high load factors. In the present study the term "optimal" when used to attribute the twist, angle of incidence or angle of attack, refers to the minimum induced drag. We intend to demonstrate that substantial differences in optimal wing twist might also occur even at two different cruise conditions and they may lead to significant penalties in induced drag for a transport airplane.

It is easy to show that only rigid wings with elliptic planform shapes (Anderson[3], 1985) achieve minimum induced drag at different lift coefficients, $C_L$ (see Appendix A). For other planforms, wing design minimizing the induced drag for one cruise condition will not guarantee minimum induced drag associated with other flight conditions. The drag penalty due to a fixed twist that is optimum only for a particular design condition may translate into operational cost compared to a tailored twist for the changing flight conditions. This drag penalty is typically small, but over the lifetime of an airplane it may translate to thousands of gallons of fuel. The objective of this paper is to investigate the magnitude of this effect so as to see if aeroelastic tailoring or other means should be considered for reducing the penalty.

Wing structural design with aeroelastic considerations, by definition, includes both structural and aerodynamic models. The aerodynamic model alone can determine the optimal total angle of incidence distribution which is in fact the sum of geometric twist as built into wing, deformation twist due to structural deformation and angle of attack. For unwsept wings, Prandtl's classical lifting line theory (LLT) can be used as a tool. Rasmussen and Smith[4] (1999) provided an easy to code derivation for the LLT as summarized in the Appendix B. Its implementation to demonstrate analytically the potential induced drag penalty is provided here in the Appendix C. Also Appendix D shows a numerical example for straight rigid wings using the LLT. For swept wings there have been efforts directly focused on wing planform optimization including twist and camber, effectively finding the optimal total angle of incidence distribution. Lamar[5] (1976) developed a code called LAMDES for this purpose. This code, has been used in number of wing design studies to date as discussed below, including the present study.

Finding the optimal total angle of incidence distribution, however, is not sufficient and systematic coupled analysis of aerodynamic and structural models are needed in designing the wing so that its geometric twist for instance, can be determined. Haftka[2] (1977) presented an optimization procedure for wing design taking drag constraints into account along with stress and strain constraints. The procedure implemented measures for the effects of load redistribution due to the flexibility of the wing structure. Craig and McLean[6] (1988) developed a computer program seeking the twist distribution and in turn spanload minimizing a combination of wing drag and weight. They used a beam structural model to evaluate the weight based on the bending strength and the Trefftz plane induced drag analysis. Iglesias and Mason[7] pointed out that because the induced drag minimum is

unconstrained, the penalty on drag is always small compared to the structural weight benefit of shifting the spanload slightly inboard compared to the elliptic distribution. Gern et al. [8] (2001) developed an aeroelastic model to consider the flexibility of the wing and aerodynamic load redistributions associated with the flight maneuvers. They used the model in sizing a strut-braced wing configuration. They considered an elliptical spanload during cruise for which the wing twist was determined by Lamar's design program LAMDES[5] (1976). This type of twist distribution is referred in this paper as the total angle of incidence at the cruise condition. Based on LAMDES result and the bending deformation, they were able to determine the jig shape (geometric twist) of the wing to be considered in other flight conditions. Gern et al.[9] (2002) implemented equivalent plate modeling for the static aeroelastic response of built-up wing structures for which aerodynamic loads were calculated by Vortex Lattice Method (VLM). They used their model to investigate the wing twist and camber tailoring or morphing via distributed actuators on the maneuver control of a lambda wing with no control surfaces. They used Lamar's wing design program LAMDES[5] (1976) for optimal total angle incidence distribution. The present paper uses the MSC.NASTRAN[10] (2002) aeroelastic module where a systematic approach is incorporated for the aeroelastic considerations in wing design.

The present study is motivated by the fact that airplanes are prone to frequent deviations from the cruise design condition during service life. For instance, on short hops they often fly below the cruise altitude for which the wing twist is determined for minimum induced drag. The objective of the paper is to demonstrate the effect of using a fixed geometric wing twist on the induced drag despite the changes in flight conditions and to make a comparison with a wing of variable twist as the flight condition changes.

The next section describes the transport wing used in this paper as an example and defines the design and off-design cruise flight conditions. The analysis section describes the aerodynamic and structural models employed and the parameters given and computed for the evaluation. Next, the four step procedure for the assessment of the drag penalty is provided. The procedure is then applied to two types of total angle of incidence distributions. Finally, concluding remarks are offered.

## II. DESCRIPTION OF THE WING AND ITS DESIGN AND OFF-DESIGN FLIGHT CONDITIONS

The induced drag was studied for an Airbus A380-like swept-tapered wing for which the parameters are given in **Table 1**.

**Table 1: Airbus A380-like swept-tapered wings for cruise speed of Mach 0.85**

| | |
|---|---|
| Wing span, $b$ (m) | 79.8 |
| Sweep at ¼ chord, $\Lambda_{1/4}$, (°) | 34.7 |
| Aspect ratio, $AR$ | 7.5 |
| Root chord, $c_r$ (m) | 16.3 |
| Tip chord, $c_t$ (m) | 4.9 |
| Taper ratio $\lambda$ | 0.3 |
| Root geometric twist, $\alpha(0)$ | 0° |

We considered two different cruise flight conditions, both at Mach 0.85, and named them the design flight condition and the off-design flight condition. The design flight condition, noted by the number 1 is the cruise flight condition for which the wing twist is determined for minimum induced drag. The lift coefficient at this cruise design condition is $C_L^{(1)}$. The off-design condition, noted by the number 2, is cruise flight at a different lift coefficient $C_L^{(2)}$. The lift coefficient associated with the design condition is considered to be higher than the off-design condition, that is $C_L^{(1)} > C_L^{(2)}$. Based on this assumption, the two possible flight condition scenarios that can be investigated are:

### A. Scenario I

Given the cruise Mach number (Mach 0.85), the cruise gross weight is identical at both flight conditions, $W^{(1)} = W^{(2)}$. The cruise altitudes, however, are different, $h^{(1)} > h^{(2)}$ which leads to a change in dynamic

pressure affecting the structural deformation. This scenario is selected to simulate the use of an aircraft on short hops for which the lower flight altitudes may be required. The altitudes in this scenario are selected as $h^{(1)} = 13100$m (43000 ft, cruise ceiling for Airbus A380) and $h^{(2)} = 10700$m (35000 ft, a typical cruise altitude that air traffic usually allows) corresponding to design condition $C_L^{(1)}$ and off-design condition $C_L^{(2)}$, respectively. The ratio of the lift coefficients $r = C_L^{(2)} / C_L^{(1)}$ is 0.7 for the selected flight Mach number and the altitudes based on air density and speed of sound variation with altitude (see Appendix D). The design and off-design condition lift coefficients are then obtained as $C_L^{(1)} = 0.6$ and $C_L^{(2)} = 0.42$ for a gross weight of $W^{(1)} = W^{(2)} =$ 420000 kg.

**B. Scenario II:**

Given the cruise Mach number (Mach 0.85), the cruise gross weight is now different considering the off-design flight has a payload less than the design case, $W^{(1)} > W^{(2)}$. For consistency with the prior scenario, we kept the lift coefficients as in scenario I. This suggests $W^{(1)} = 420000$ kg., and $W^{(2)} = 294000$ kg (ratio is kept at 0.7). Note that for reduced cruise weight, minimizing the power requires higher altitude as shown in **Figure 1**. The altitude, however, may be limited due to other design considerations such as fuselage design limits, or air traffic rules. This scenario is intended to simulate such limitations and so the design and off-design cruise altitudes are kept the same, that is $h^{(1)} = h^{(2)}$=13100 m. The two scenarios are summarized in **Table 2**.

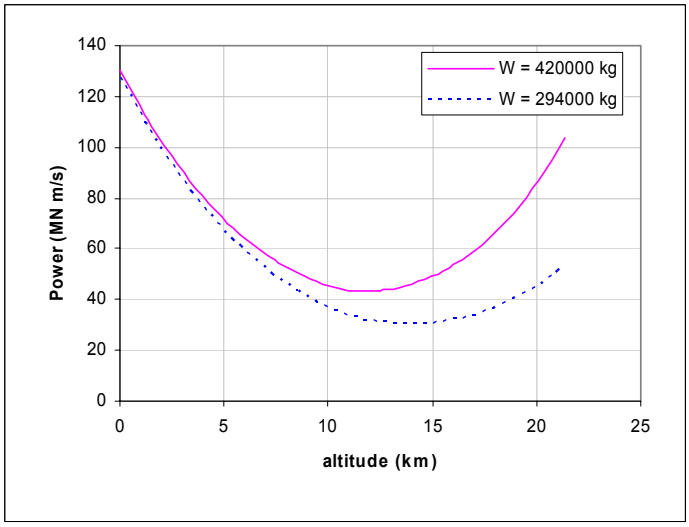


**Figure 1: Power required as a function of altitude at different cruise weight**

**Table 2: Summary of Scenario I and Scenario II**

| | Scenario I | Scenario II |
|---|---|---|
| Flight Mach number, $M^{(1)} = M^{(2)}$ | 0.85 | 0.85 |
| Lift coefficient, $C_L^{(1)}$ / $C_L^{(2)}$ | 0.6 / 0.42 | 0.6 / 0.42 |
| Altitude (m) $h^{(1)}$ / $h^{(2)}$ | 13100 / 10700 | 13100 / 13100 |
| Dynamic pressure (Pa), $Q^{(1)}$ / $Q^{(2)}$ | 8212 / 12058 | 8212 / 8212 |
| Cruise weight (kg), $W^{(1)}$ / $W^{(2)}$ | 420000 / 420000 | 420000 / 294000 |

## III. ANALYSIS

The effect of a fixed geometric wing twist on the induced drag at different flight conditions is assessed by studying the span efficiency factor *e.* It determines the induced drag coefficient of a wing of aspect ratio $AR$ for a given lift coefficient $C_L$ as in Eq. (1),

$$C_{D_i} = \frac{C_L^2}{e\pi AR}. \tag{1}$$

### A. Aerodynamic Model:

The aeroelasticity module of MSC.NASTRAN (2002) was used for the aerodynamic computations (Doublet-Lattice subsonic lifting surface), the structural analyses and optimization of the swept wing. The aerodynamic model employs a mesh of $N_{chord}$ x $N_{span}$ ( $N_{chord}$ and $N_{span}$ are the number of aerodynamic panels chordwise and spanwise, respectively). A representative sketch of the aerodynamic model is shown in **Figure 2**.

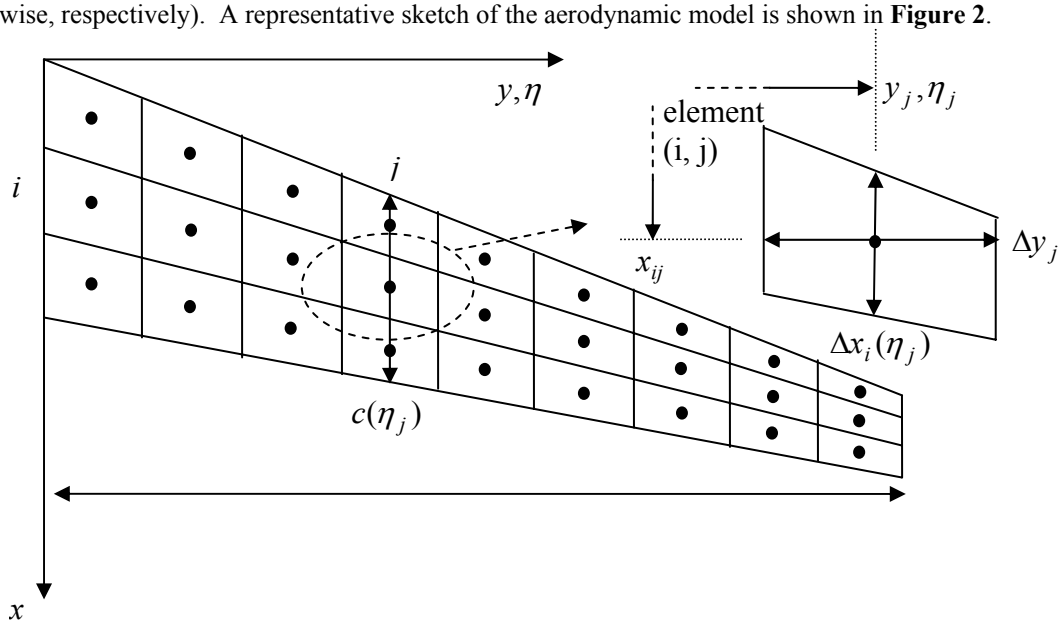


**Figure 2: Aerodynamic NASTRAN model description for the swept-tapered wing**

The width of all the aerodynamic boxes, $\Delta y_j$ is constant. The length of the aerodynamic boxes along the chord is constant, but it varies along the span due to taper ratio. In this study we used $N_{chord} = 8$ and $N_{span} = 50$ for the aerodynamic model. No camber is included, so the total geometric angle of incidence $\alpha_{tot}(\eta)$ is constant along the chord at a given spanwise station $\eta$ and determined by the angle of attack, $\overline{\alpha}$ and the geometric wing twist distribution over the wing span, $\alpha(\eta)$. The wing geometric twist distribution is implemented into the aerodynamic model by DMI (Direct Matrix Input) entries in NASTRAN and the angle of attack is specified in the TRIM bulk data entry.

The aeroelastic module of MSC.NASTRAN (2002) reports the net aerodynamic pressure coefficients at each box center, $c_p^{(ij)}$. This information was converted into the span efficiency factor *e* and the total lift coefficient $C_L$ using the FORTRAN code LIDRAG. This program computes the span efficiency factor *e* for a single planar lifting surface from the spanload using a Fast Fourier Transform. The spanload required by the program is

$$c_{span}(\eta_j) = \frac{c(\eta_j)c_l(\eta_j)}{c_{av}}, \tag{2}$$

where $\eta_j = \frac{y_j}{b/2}$ and $c_{av}$ is the average chord length. The local lift coefficient $c_l(\eta_j)$ is found from the pressure coefficients $c_p^{(ij)}$ as

$$c_l(\eta_j) = \frac{\sum_{i=1}^{N_{chord}} c_p^{(ij)} \Delta x_i(\eta_j)}{c(\eta_j)} \quad . \tag{3}$$

**B. Structural Model:**

The structure of the wing was modeled as a hexagonal wing box which consists of leading and trailing edge spars and fifteen equally spaced ribs. The upper and lower skins of the wing box are modeled by 28 quadrilateral shell elements each. The spar webs and cap areas are modeled by shear elements (14 each) and the rod elements (14 upper and 14 lower each), respectively. Each rib is divided into two shear webs modeled by shear elements (total 30) whose circumference was supported by rod elements. Clamped boundary conditions were applied at the root of the wing. Figure 3 shows the half-span model and a blowout view of a wing box bay. The material properties used in the model are given in **Table 3**.

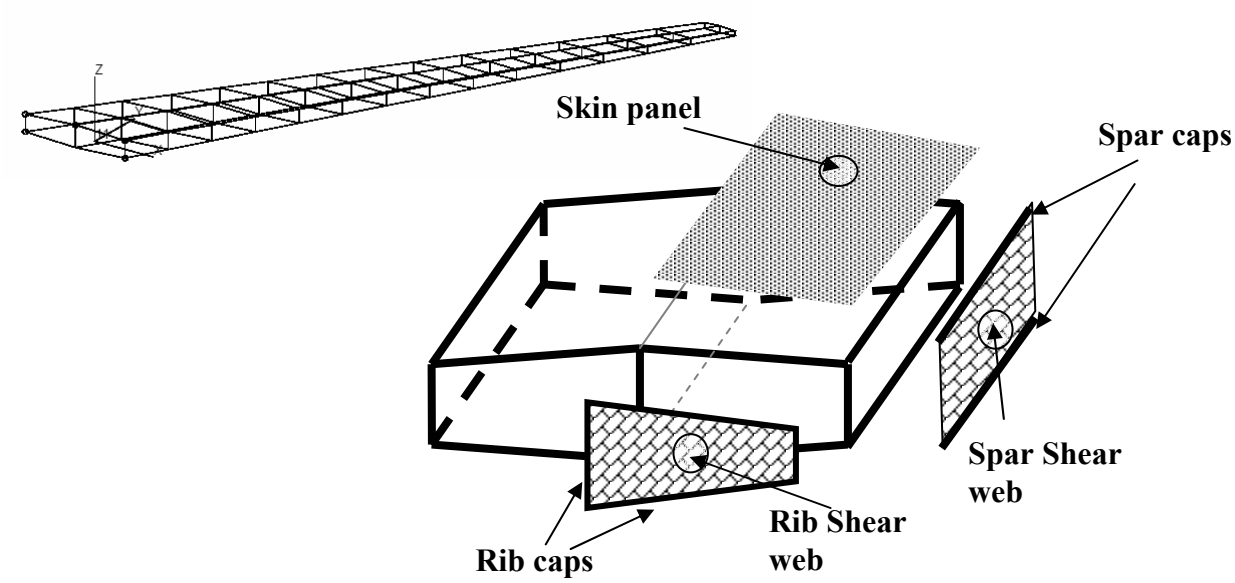


**Figure 3: Structural NASTRAN model for hexagonal wing box of the swept-tapered wing**

**Table 3: Properties for the wing material**

| | |
|---|---|
| Young's modulus, $E$ (GPa) | 70 |
| Poison's ratio, $\nu$ | 0.33 |
| Allowable stress, $\sigma_{all}$ (MPa) | 489 |
| Density, $\rho$ (kg/m$^3$) | 2769 |

The upper and lower skins are considered to be identical, and each bay from root to tip assigns one variable for structural optimization, for a total of 14 skin panel thicknesses as variables. The structural optimization where we minimize the weight and impose only stress constraints used a load factor of 2.5 on the dynamic pressure and a safety factor of 1.5 on the stress allowable.

### C. Parameters to report

The induced drag and the span efficiency factor are determined by the total spanwise angle of incidence distribution, $\alpha_{tot}(\eta)$. The distribution at a flight condition is the sum of the geometric twist $\alpha(\eta)$, twist change due to structural deformation $\alpha_{def}(\eta)$ and the angle of attack $\overline{\alpha}$. Figure 4 shows the wing twist, angle of attack and total angle of incidence at a spanwise station $\eta$. The deformation twist or the twist change due to structural deformation $\alpha_{def}(\eta)$ depends on the geometric twist and the angle of attack, that is $\alpha_{def}(\alpha(\eta), \overline{\alpha})$. The sum of $\alpha(\eta)$ and $\alpha_{def}(\eta)$ is what we refer to here as elastic wing twist, $\alpha_{elas}(\eta)$. The elastic wing twist and total angle of incidence distribution are expressed as in Eq. (4),

$$\begin{aligned} \alpha_{elas}(\eta) &= \alpha(\eta) + \alpha_{def}(\eta), \\ \alpha_{tot}(\eta) &= \alpha_{elas}(\eta) + \overline{\alpha} \end{aligned} \quad . \tag{4}$$

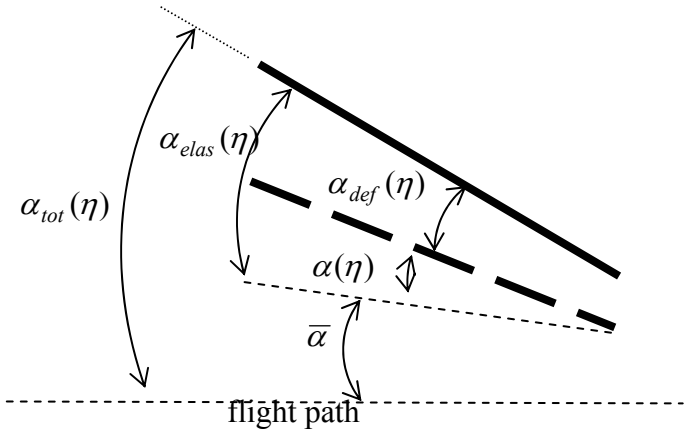


**Figure 4: Schematic for wing twist and total angle of incidence**

Note that the geometric twist at the root is set to be zero, $\alpha_{root} = \alpha(0) = 0^\circ$ as given in **Table 1**. This also suggests that the total angle of incidence at the root is equal to the angle of attack for a clamped wing due to Eq. (4),

$$\overline{\alpha} = \alpha_{tot}(0) \tag{5}$$

**Table 4** summarizes the parameters defining the cruise flight conditions and the parameters to be determined through the procedure followed in the wing example presented here. The second and third columns define the optimal wing associated with the design and off-design flight conditions, respectively. The last column shows the parameters at the off-design flight condition, but with the optimal geometric wing twist of design flight condition. The difference in span efficiency between the third and the last columns provides the induced drag penalty due to flight at off-design condition. This is the penalty that may be recovered by aeroelastic tailoring or other means of changing the twist distribution at different flight conditions.

## IV. PROCEDURE

The overall procedure to evaluate the induced drag penalty associated with the fixed geometric twist consists of several steps. This section introduces the generic descriptions of these steps that were followed for two specific examples of total angle of incidence distributions. Recall that the term "optimal" when used to attribute the twist, angle of incidence or angle of attack, refers to the minimum induced drag.

### A. STEP 1: Optimal total angle of incidence via Aerodynamic Analyses:

The goal in the present paper requires assessing the performance of the optimal geometric wing twist for the design condition at the off-design condition. As the overall procedure demonstrates, this assessment can be done by comparing the total angle of incidence distributions since they are the sum of the geometric and deformation twists

and the angle of attack, Eq. (4). Note that the optimal total angle of incidence for minimum induced drag at a given flight condition is invariant and can be determined as if the wing is rigid. That is, $\alpha_{tot}(\eta)\big|_{opt}$ and the optimal angle of attack ($\overline{\alpha}_{opt} = \alpha_{tot}(0)\big|_{opt}$) can be found by aerodynamic analyses alone. This is done for the given planform at both design and off-design flight conditions, lift coefficients $C_L^{(1)}$ and $C_L^{(2)}$, respectively. This step determines $\alpha_{tot}^{(1)}(\eta)\big|_{opt}$, $\overline{\alpha}_{opt}^{(1)}$ and $e_{\max}^{(1)}$ for design condition and $\alpha_{tot}^{(2)}(\eta)\big|_{opt}$, $\overline{\alpha}_{opt}^{(2)}$ and $e_{\max}^{(2)}$ for off-design condition. For a rigid wing, the total angle of incidence gives the rigid wing geometric twist, denoted here by $\alpha(\eta)\big|_{rigid}$, since the deformation twist is zero along the span. The design optimal geometric twist for the rigid wing is,

$$\alpha_{opt}^{(1)}(\eta)\Big|_{rigid} = \alpha_{tot}^{(1)}(\eta)\Big|_{opt} - \overline{\alpha}_{opt}^{(1)}. \tag{6}$$

**Table 4: Parameters to determine at the design and off-design conditions**

| | Design condition (1) Optimal wing | Off-design condition (2) Optimal wing | Off-design condition (2) Non-optimal wing |
|---|---|---|---|
| Lift coefficient, $C_L$ | $C_L^{(1)}$ | $C_L^{(2)}$ | $C_L^{(2)}$ |
| Altitude, $h$ | $h^{(1)}$ | $h^{(2)}$ | $h^{(2)}$ |
| Dynamic Pressure, $Q$ | $Q^{(1)}$ | $Q^{(2)}$ | $Q^{(2)}$ |
| Cruise weight | $W^{(1)}$ | $W^{(2)}$ | $W^{(2)}$ |
| Geometric Wing twist, $\alpha(\eta)$ | $\alpha_{opt}^{(1)}(\eta)$ | $\alpha_{opt}^{(2)}(\eta)$ | $\alpha_{opt}^{(1)}(\eta)$ |
| Angle of attack, $\overline{\alpha}$ | $\overline{\alpha}_{opt}^{(1)}$ | $\overline{\alpha}_{opt}^{(2)}$ | $\overline{\alpha}^{(2)}$ |
| Deformation twist, $\alpha_{def}(\alpha(\eta),\overline{\alpha})$ | $\alpha_{def}(\alpha_{opt}^{(1)}(\eta),\overline{\alpha}_{opt}^{(1)})$ | $\alpha_{def}(\alpha_{opt}^{(2)}(\eta),\overline{\alpha}_{opt}^{(2)})$ | $\alpha_{def}(\alpha_{opt}^{(1)}(\eta),\overline{\alpha}^{(2)})$ |
| Elastic wing twist, $\alpha_{elas}(\eta)$ | $\alpha_{elas}^{(1)}(\eta)\big\|_{opt} = \alpha_{opt}^{(1)}(\eta) + \alpha_{def}(\alpha_{opt}^{(1)}(\eta),\overline{\alpha}_{opt}^{(1)})$ | $\alpha_{elas}^{(2)}(\eta)\big\|_{opt} = \alpha_{opt}^{(2)}(\eta) + \alpha_{def}(\alpha_{opt}^{(2)}(\eta),\overline{\alpha}_{opt}^{(2)})$ | $\alpha_{elas}^{(2)}(\eta)\big\|_{non} = \alpha_{opt}^{(1)}(\eta) + \alpha_{def}(\alpha_{opt}^{(1)}(\eta),\overline{\alpha}^{(2)})$ |
| Total Angle of Incidence, $\alpha_{tot}(\eta)$ | $\alpha_{tot}^{(1)}(\eta)\big\|_{opt} = \alpha_{elas}^{(1)}(\eta)\big\|_{opt} + \overline{\alpha}_{opt}^{(1)}$ | $\alpha_{tot}^{(2)}(\eta)\big\|_{opt} = \alpha_{elas}^{(2)}(\eta)\big\|_{opt} + \overline{\alpha}_{opt}^{(2)}$ | $\alpha_{tot}^{(2)}(\eta)\big\|_{non} = \alpha_{elas}^{(2)}(\eta)\big\|_{non} + \overline{\alpha}^{(2)}$ |
| Span efficiency, $e$ | $e_{\max}^{(1)}$ | $e_{\max}^{(2)}$ | $e^{(2)}$ |
| Induced drag penalty | | $\dfrac{e_{\max}^{(2)} - e^{(2)}}{e_{\max}^{(2)}}$ | |

**B. STEP 2: Induced drag penalty for the design condition optimal wing operating at the off-design condition when structural deformation is excluded (no deformation twist:)**

This is an intermediate step to see if there is an induced drag penalty even if the structural deformation is not included in the evaluation. The off-design condition is achieved by keeping the optimal geometric twist for the design condition, but changing the angle of attack. That is, given the planform and geometric twist distribution $\alpha_{opt}^{(1)}(\eta)\Big|_{rigid}$, several angles of attack, $\overline{\alpha}_i$ are used in the aerodynamic analyses for $C_L$, so that $\overline{\alpha}^{(2)}$ associated with $C_L^{(2)}$ may be found by interpolation. The alternative to the optimal total angle of incidence $\alpha_{tot}^{(2)}(\eta)\Big|_{opt}$ is now $\alpha_{tot}^{(2)}(\eta) = \alpha_{opt}^{(1)}(\eta)\Big|_{rigid} + \overline{\alpha}^{(2)}$ and the respective span efficiency factors $e_{\max}^{(2)}$ and $e^{(2)}$ are compared to see how much the drag can be improved if the wing shape can change to the optimal in flight.

**C. STEP 3: Change of deformation twist as a function of the flight condition:**

The deformation twist for a given geometric twist $\alpha(\eta)$ and dynamic pressure $Q$ at an angle of attack $\overline{\alpha}$ is denoted as $\alpha_{def}(\alpha(\eta), Q, \overline{\alpha})$ and expressed here as in Eq. (7),

$$\alpha_{def}(\alpha(\eta), Q, \overline{\alpha}) = \sin^{-1}\left(\frac{w_{LE}(\eta) - w_{TE}(\eta)}{c(\eta)}\right). \tag{7}$$

where $w_{LE}(\eta), w_{TE}(\eta)$ and $c(\eta)$ are the lateral displacements at the leading and trailing edges and the chord length at the spanwise station $\eta$, respectively (see **Figure** 5). The lateral displacements are obtained by NASTRAN aeroelastic analysis.

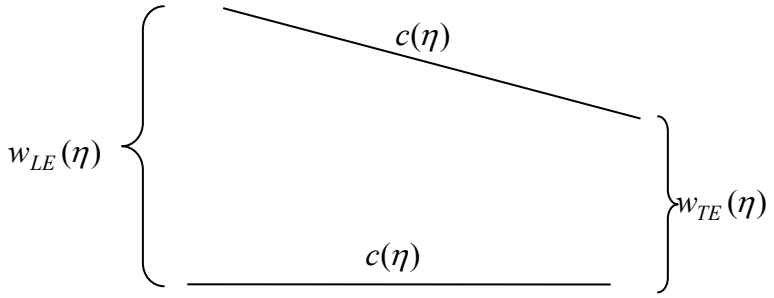


**Figure** 5**: Lateral displacements at spanwise station** $\eta$

The optimum total angle of incidence distribution and angle of attack for the design condition from STEP 1 $\alpha_{tot}^{(1)}(\eta)\Big|_{opt}$ and $\overline{\alpha}_{opt}^{(1)}$, respectively, are indeed the solution even for the flexible wing at the design dynamic pressure, $Q^{(1)}$. This is because the structural deformation is normally compensated for (jig-shape correction) by changing the geometric twist from optimal geometric twist of the rigid wing Eq. (6). That is, the elastic wing twist is equal to the optimal geometric twist from step 1 Eq. (6), that is obtained if the wing was rigid,

$$\alpha_{elas}^{(1)}(\eta) = \alpha_{opt}^{(1)}(\eta)\Big|_{rigid}. \tag{8}$$

Then, Eqs. (4) and (8) yield that, the optimal geometric twist of the flexible wing of the design condition is,

$$\alpha_{opt}^{(1)}(\eta) = \alpha_{opt}^{(1)}(\eta)\Big|_{rigid} - \alpha_{def}(\alpha_{opt}^{(1)}(\eta), Q^{(1)}, \overline{\alpha}_{opt}^{(1)}). \tag{9}$$

The optimal geometric wing twist for the design condition $\alpha_{opt}^{(1)}(\eta)$ will result in a different total angle of incidence distribution $\alpha_{tot}(\eta)$ at an off-design condition. This is because the structural deformation is different for

different lift coefficients associated with different angle of attack at the off-design dynamic pressure $Q^{(2)}$. The change in the deformation twist at an angle of attack $\overline{\alpha}_i$ can be expressed as in Eq. (10),

$$\Delta\alpha_i(\eta) = \alpha_{def}(\alpha_{opt}^{(1)}(\eta), Q^{(1)}, \overline{\alpha}_{opt}^{(1)}) - \alpha_{def}(\alpha_{opt}^{(1)}(\eta), Q^{(2)}, \overline{\alpha}_i). \tag{10}$$

Note that the optimal geometric twist $\alpha_{opt}^{(1)}(\eta)$ used in Eq. (10) is not known, and it requires an iterative procedure due to Eq. (9). Instead, we determine the difference between the deformation twists by using the optimal geometric twist of the rigid wing analysis from step 2,

$$\Delta\alpha_i(\eta) = \alpha_{def}(\alpha_{opt}^{(1)}(\eta)\Big|_{rigid}, Q^{(1)}, \overline{\alpha}_{opt}^{(1)}) - \alpha_{def}(\alpha_{opt}^{(1)}(\eta)\Big|_{rigid}, Q^{(2)}, \overline{\alpha}_i). \tag{11}$$

The goal here is to find the how much the total angle of incidence distribution is distorted by the difference in the structural deformation at the design and off-design conditions as given in Eq. (12)

$$\alpha_{tot}(\eta)\Big|_{\overline{\alpha}_i} = \alpha_{tot}^{(1)}(\eta)\Big|_{opt} - \Delta\alpha_i(\eta) \tag{12}$$

In short, step 3 is: given the optimal geometric twist of the rigid wing $\alpha_{opt}^{(1)}(\eta)\Big|_{rigid}$, optimal angle of attack $\overline{\alpha}_{opt}^{(1)}$ and dynamic pressures $Q^{(1)}$ and $Q^{(2)}$, using Eq. (11) and (12) respectively, calculate the change in deformation twist and the total angle of incidence for several angles of attack at the off-design dynamic pressure by aeroelastic analyses.

**D. STEP 4: Induced drag penalty for the design-condition optimal wing operating at the off-design condition when structural deformation is also included:**

Given the total angle of incidence $\alpha_{tot}(\eta)\Big|_i$ at angle of attack $\overline{\alpha}_i$ from step 3, aerodynamic analyses alone are performed to evaluate the lift coefficient $C_L\big|_{\alpha_i}$. The interpolation for the $C_L\big|_{\alpha_i}$ versus $\overline{\alpha}_i$ finds the angle of attack $\overline{\alpha}^{(2)}$ giving the off-design lift coefficient $C_L^{(2)}$. Step 3 is then repeated for verification for the target lift coefficient $C_L^{(2)}$ with $\overline{\alpha}_i = \overline{\alpha}^{(2)}$ and the total angle of incidence at the off-design condition is determined as $\alpha_{tot}^{(2)}(\eta) = \alpha_{tot}(\eta)\Big|_{\overline{\alpha}^{(2)}}$ by Eq. (12). The drag penalty for the flexible wing is calculated by comparing the optimal total angle of incidence distribution $\alpha_{tot}^{(2)}(\eta)\Big|_{opt}$ from step 1 and the total angle of incidence distribution $\alpha_{tot}^{(2)}(\eta)$ at step 4. This step is basically the same as step 2, except that the total angle of incidence of the off-design condition is determined by the step 4.

## V. INDUCED DRAG PENALTY FOR AEROELASTIC WING

The procedure described by these four steps is applied to two types of optimal total angle of incidence distributions in the present study: ED Type: Wing of total angle of incidence distribution to obtain near elliptic spanload and the minimum induced drag, and SLW Type: Wing of straight-line wrapped total angle of incidence distribution. The results for the two types of wing through the steps are presented in this section. **Figure 6** summarizes procedure as a flowchart.

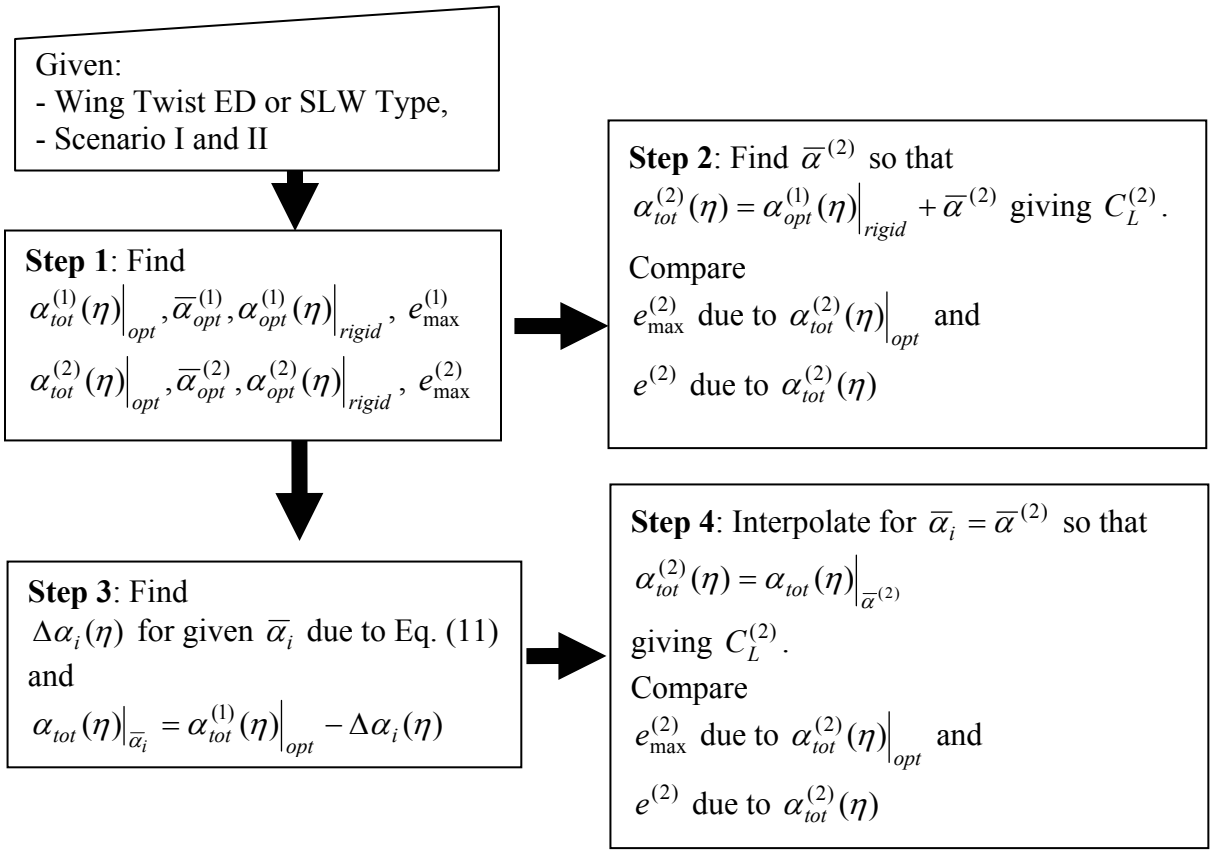


**Figure** 6**: Flowchart for the procedure followed in induced drag penalty evaluation**

***A.* ED Type: Wing of total angle of incidence distribution to obtain elliptic spanload *and the minimum induced drag.***

*Step 1*

For the wing of **Table 1**, LAMDES due to Lamar (1986) was used to find the optimal total angle of incidence distribution $\alpha_{tot}^{(1)}(\eta)\big|_{opt}$ offering elliptic spanload for both $C_L^{(1)} = 0.6$ and $C_L^{(2)} = 0.42$. For design and off-design flight conditions the angles of attack, Eq. (5) were computed as $\overline{\alpha}_{opt}^{(1)} = 7.63^\circ$ and $\overline{\alpha}_{opt}^{(2)} = 5.35^\circ$, respectively. The geometric twist of the rigid wing $\alpha_{opt}^{(1)}(\eta)\big|_{rigid}$ and $\alpha_{opt}^{(2)}(\eta)\big|_{rigid}$ are shown in **Figure** 7 using the LAMDES output and Eq. (6). The spanwise geometric twist of the rigid wing and the angle of attack, that is the total incidence distribution for the designs were included in the MSC.NASTRAN input file for each design. Aerodynamic analyses by NASTRAN (rigid wing) were performed and the results were post-processed via LIDRAG for the span efficiency factors, and corresponding to and. The results are summarized in the second and third columns of Table 5.

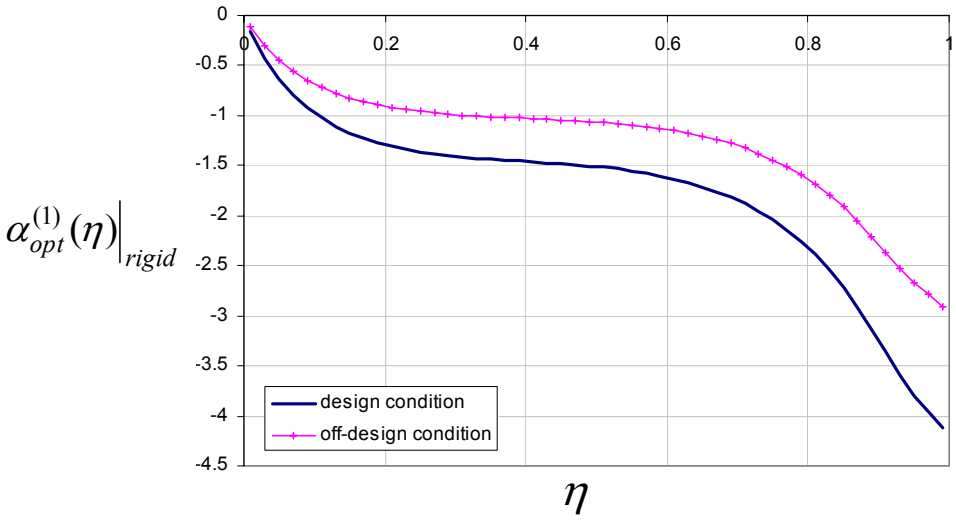


**Figure 7: ED Type Rigid wing optimal geometric twist distribution by LAMDES for design and off-design flight conditions, $\alpha_{opt}^{(1)}(\eta)\big|_{rigid}$ ($\overline{\alpha}_{opt}^{(1)} = 7.63^\circ$) and $\alpha_{opt}^{(2)}(\eta)\big|_{rigid}$ ($\overline{\alpha}_{opt}^{(2)} = 5.35^\circ$)**

*Step 2:*

We found the angle of attack $\overline{\alpha}^{(2)}$ that generates the off-design condition $C_L^{(2)} = 0.42$ when we use the geometric twist of design condition, $\alpha_{opt}^{(1)}(\eta)\big|_{rigid}$ as shown in the last column of the **Table 5**.

**Table 5: Rigid wing analyses for ED Type distribution $\alpha_{tot}(\eta)$: Effect of constant angle of attack adjustment on drag optimum swept-tapered wing for $C_L^{(1)} = 0.6$.**

| | Design condition (1) Optimal wing | Off-design condition (2) Optimal wing | Off-design condition (2) Non-optimal wing |
|---|---|---|---|
| Lift coefficient, $C_L$ | $C_L^{(1)} = 0.6$ | $C_L^{(2)} = 0.42$ | $C_L^{(2)} = 0.42$ |
| Geometric twist, $\alpha(\theta)$ | $\alpha_{opt}^{(1)}(\eta)\big\|_{rigid}$ | $\alpha_{opt}^{(2)}(\eta)\big\|_{rigid}$ | $\alpha_{opt}^{(1)}(\eta)\big\|_{rigid}$ |
| Angle of attack, $\overline{\alpha}$ | $\overline{\alpha}_{opt}^{(1)} = 7.63^o$ | $\overline{\alpha}_{opt}^{(2)} = 5.35^o$ | $\overline{\alpha}^{(2)} = 5.77^o$ |
| Span efficiency, $e$ | $e_{\max}^{(1)} = 0.99736$ | $e_{\max}^{(2)} = 0.99738$ | $e^{(2)} = 0.99884$ |
| Induced drag coefficient, $C_{D_i}$ | 0.01539 | 0.00751 | 0.00749 |
| Induced drag penalty | | $\frac{e_{\max}^{(2)} - e^{(2)}}{e_{\max}^{(2)}} = -0.004$ | |

Comparing the last two columns of the **Table 5**, we can note that the optimal geometric twist for the design condition resulted in a higher span efficiency factor at the off-design condition than the off-design twist via LAMDES, that $e^{(2)} > e_{\max}^{(2)}$ suggesting no drag penalty. This is attributed to the fact that LAMDES does not find

the true optimum or true elliptic spanload, but near optimal. Twist $\alpha_{opt}^{(2)}(\eta)\Big|_{rigid}$ and $\overline{\alpha}_{opt}^{(2)} = 5.35^{o}$ happened to be worse than the adjusted or shifted twist, $\alpha_{opt}^{(1)}(\eta)\Big|_{rigid}$ and $\overline{\alpha}^{(2)} = 5.77^{o}$. Therefore we consider for the rest of the procedure $\alpha_{opt}^{(2)}(\eta)\Big|_{rigid} = \alpha_{opt}^{(1)}(\eta)\Big|_{rigid}$ and $\overline{\alpha}_{opt}^{(2)} = \overline{\alpha}^{(2)} = 5.77^{o}$.

*Step 3:*

The lift coefficient of the off-design conditions as a function of the angle of attack, are shown in **Figure** 8 and **Figure** 9, respectively for the Scenario I and Scenario II.

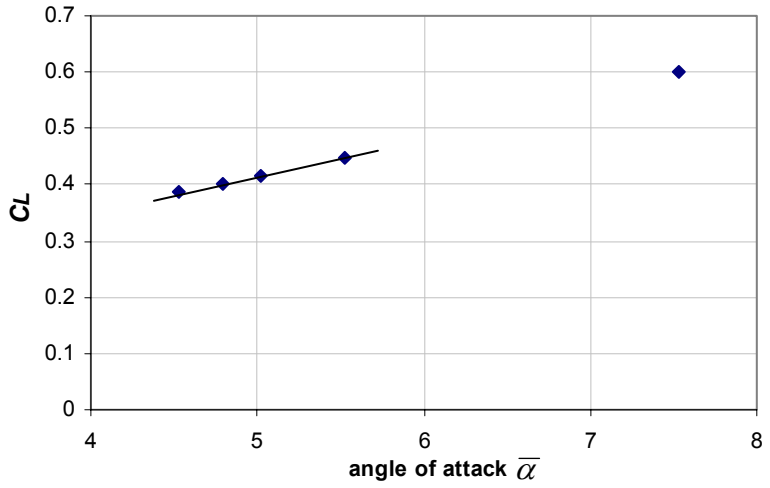


**Figure** 8**: ED Type, Scenario I: The lift coefficient versus angle of attack after step 3**

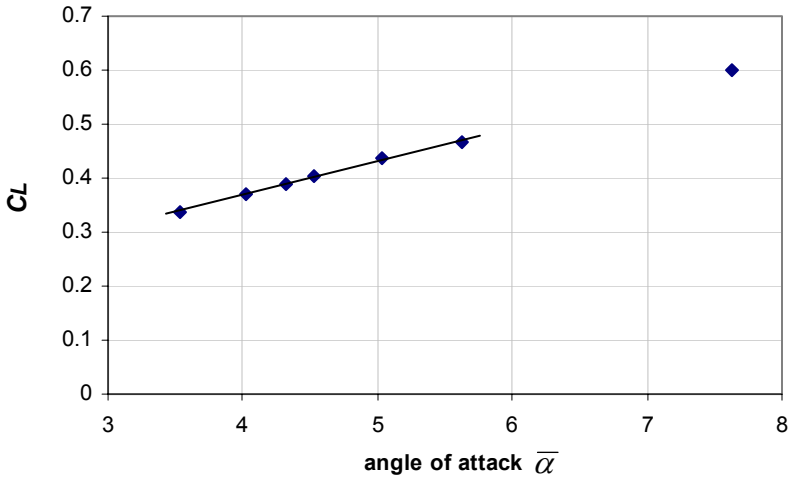


**Figure** 9**: ED Type, Scenario II: The lift coefficient versus angle of attack after step 3**

*Step 4:*

From the data generated in step 3 the angle of attack for Scenario I was determined, $\overline{\alpha}^{(2)}\Big|_{I} = 5.08^{\circ}$ and for scenario II $\overline{\alpha}^{(2)}\Big|_{II} = 4.80^{\circ}$, both associated with the target off-design lift coefficient $C_L^{(2)}$=0.42. Recall that

$\alpha_{tot}^{(2)}(\eta) = \alpha_{tot}(\eta)\Big|_{\overline{\alpha}^{(2)}}$, and so the total angle of incidence distributions for the optimal case, scenario I and scenario II of the off-design condition can now be sown as in **Figure** 10. Spanloads associated with the off-design condition optimal wing and two non-optimal settings based on optimal design condition wing (Scenario I and II) are shown in **Figure** 11.

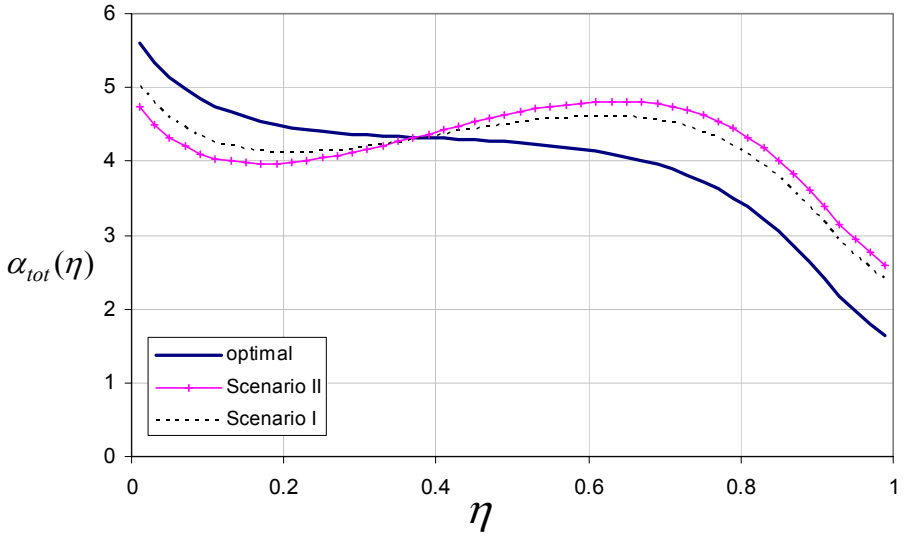


**Figure** 10**: ED Type, comparison of total angle of incidence, $\alpha_{tot}(\eta)$ : Optimal wing for off-design condition versus the non-optimal wings**

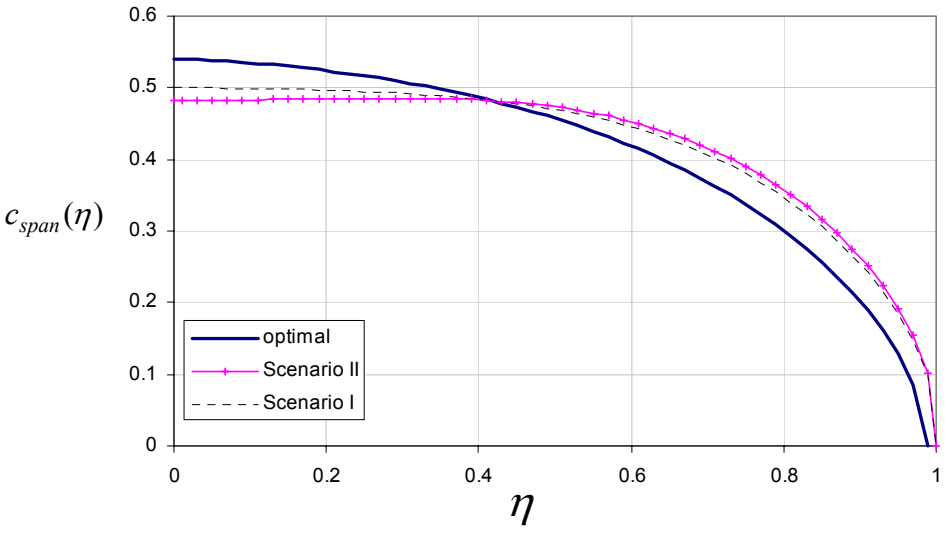


**Figure** 11**: ED Type, spanload comparison, $c_{span}(\eta)$ : Optimal wing for off-design condition versus the non-optimal wings**

Finally **Table 6** summarizes the results for the induced drag penalty for the ED Type case. The second column presents the optimal wing for the design condition. The third column shows the optimal wing of off-design flight condition and this is considered as the wing tailored for the off-design conditions. Note that these columns correspond to the optimal wings determined in Step 1 and 2 . The fourth and fifth columns present the results

(Scenario I and II, respectively) for the optimal wing of design condition that with an angle of attack adjustment to achieve the off-design flight condition. Therefore, the induced drag penalty can be determined by comparing column three with the last two columns. For Twist A in Scenario I there is about a 1% reduction in the span efficiency factor that corresponds to about a one drag-count increase. For the Scenario II, the span efficiency is reduced by 2%, and the there is an increase of two drag-counts.

**Table** 6**: Effect of constant angle of attack adjustment on drag optimum swept-tapered wing of Twist A for** $C_L^{(1)} = 0.6$ **.**

| | Design [1] Optimal wing | Off-design [2] Optimal wing | Off-design [2] Non-optimal wing Scenario I | Off-design [2] Non-optimal wing Scenario II |
|---|---|---|---|---|
| Lift coefficient, $C_L$ | $C_L^{(1)} = 0.60$ | $C_L^{(2)} = 0.42$ | $C_L^{(2)} = 0.42$ | $C_L^{(2)} = 0.42$ |
| Total angle of incidence, $\alpha_{tot}(\eta)$ | $\alpha_{tot}^{(1)}(\eta)\big\|_{opt}$ | $\alpha_{tot}^{(2)}(\eta)\big\|_{opt}$ | $\alpha_{tot}^{(2)}(\eta) = \alpha_{tot}(\eta)\big\|_{\bar{\alpha}^{(2)}}$ | $\alpha_{tot}^{(2)}(\eta) = \alpha_{tot}(\eta)\big\|_{\bar{\alpha}^{(2)}}$ |
| Angle of attack, $\bar{\alpha}$ | $\bar{\alpha}_{opt}^{(1)} = 7.63^{\circ}$ | $\bar{\alpha}_{opt}^{(2)} = 5.77^{\circ}$ | $\bar{\alpha}^{(2)}\big\|_I = 5.08^{\circ}$ | $\bar{\alpha}^{(2)}\big\|_{II} = 4.80^{\circ}$ |
| Span efficiency, *e* | $e_{\max}^{(1)} = 0.99736$ | $e_{\max}^{(2)} = 0.99884$ | $e^{(2)} = 0.98912$ | $e^{(2)} = 0.97922$ |
| Induced drag coefficient, $C_{D_i}$ | 0.01539 | 0.00749 | 0.00758 | 0.00766 |
| Induced drag penalty, $\frac{e_{\max}^{(2)} - e^{(2)}}{e_{\max}^{(2)}}$ | | | 0.01 | 0.02 |

**B. SLW Type: Wing of straight-line wrapped total angle of incidence distribution**

The total angle of incidence for a wing with straight-line wrapped surfaces was also considered. That is, the wing made of surfaces that are straight between spanwise control stations. The distribution along the span due to this constraint may be obtained by pure geometry and the distribution is expressed as the following,

$$\alpha_{tot}(\eta) = \sin^{-1}\left[\frac{\sin\alpha_{root} + \left(\lambda\sin\alpha_{tip} - \sin\alpha_{root}\right)\eta}{1-(1-\lambda)\eta}\right], \tag{13}$$

where $\alpha_{root} = \alpha_{tot}(0) = \bar{\alpha}$ and $\alpha_{tip} = \alpha_{tot}(1)$ are total angle of incidence at the root (the angle of attack) and tip, respectively. Equation (13) is applicable to both unswept and swept wings. Straight-line wrapping or ruled surfaces are desired to reduce manufacturing cost. This constraint may practically be needed while the wing is mounted on the jig rather than for the total angle of incidence distribution. It was, however, considered here so that sensitivity of the drag penalty to the type of distribution could also be investigated.

*Step1:*

For the wing of **Table 1**, straight-line wrapped surfaces were considered for total angle of incidence at the root $\alpha_{root}$ (equal to angle of attack) and at the tip $\alpha_{tip}$ in the range of 4º–8º and 0º–4º, respectively. Nine combinations generating a Faced Centered Composite Design (FCCD) were studied first (see **Table 7**). The spanwise total angle of incidence distributions for the designs were obtained by using Eq. (13) and included in the MSC.NASTRAN

input file for each design. Aerodynamic MSC.NASTRAN analyses followed by post-processing via LIDRAG generated the results as reported in **Table 7**.

**Table 7: NASTRAN analysis results post-processed by LIDRAG for span efficiency factor and total lift coefficient.**

| FCCD | | Taper ratio $\lambda = 0.3$ | |
|---|---|---|---|
| $\alpha_{root}$ | $\alpha_{tip}$ | $e$ | $C_L$ |
| 4 | 0 | 0.97779 | 0.310 |
| 6 | 0 | 0.97774 | 0.465 |
| 8 | 0 | 0.97767 | 0.619 |
| 4 | 2 | 0.99710 | 0.350 |
| 6 | 2 | 0.99672 | 0.505 |
| 8 | 2 | 0.99447 | 0.660 |
| 4 | 4 | 0.97529 | 0.391 |
| 6 | 4 | 0.99299 | 0.546 |
| 8 | 4 | 0.99710 | 0.700 |

Next, using the data of **Table 7**, we generated quadratic response surface approximations $\hat{e}(\alpha_{root}, \alpha_{tip})$ and $\hat{C}_L(\alpha_{root}, \alpha_{tip})$ for span efficiency factor $e$ and the total lift coefficient $C_L$, respectively. Coefficient of variations suggested that the response surfaces are accurate, about 0.5% for $\hat{e}(\alpha_{root}, \alpha_{tip})$ and about 0.1% for $\hat{C}_L(\alpha_{root}, \alpha_{tip})$. The response surfaces can now be used to predict the span efficiency factor and the lift coefficient for a given $\alpha_{root}$ and $\alpha_{tip}$ within their ranges, (4º – 8º) and (0º – 4º), respectively.

The response surfaces were implemented in the EXCEL Solver to find $\alpha_{root}$ (angle of attack $\overline{\alpha}$) and $\alpha_{tip}$ defining the optimal total angle of incidence distribution $\alpha_{tot}^{(1)}(\eta)\Big|_{opt}$ for maximum span efficiency factor associated with $C_L^{(1)} = 0.6$ and $C_L^{(2)} = 0.42$. The optimal angles of attack and the tip incidence, were found for design flight condition as $\overline{\alpha}_{opt}^{(1)} = \alpha_{root}^{(1)} = 7.07^\circ$, $\alpha_{tip}^{(1)}\Big|_{opt} = 2.60^\circ$ and for off-design flight conditions as $\overline{\alpha}_{opt}^{(2)} = \alpha_{root}^{(2)} 4.89^\circ$, $\alpha_{tip}^{(2)}\Big|_{opt} = 2.05^\circ$. The geometric twist of the rigid wing $\alpha_{opt}^{(1)}(\eta)\Big|_{rigid}$ and $\alpha_{opt}^{(2)}(\eta)\Big|_{rigid}$ are shown in **Figure** 7 using the Eq. (6) and (13). The spanwise geometric twist of the rigid wing and the angle of attack, were included in the NASTRAN input file for each design. Aerodynamic alone analyses by NASTRAN (rigid wing) were performed and the results were post-processed via LIDRAG for the span efficiency factors, $e_{\max}^{(1)}$ and $e_{\max}^{(2)}$ corresponding to $C_L^{(1)} = 0.6$ and $C_L^{(2)} = 0.42$. The results are summarized in the second and third columns of **Table 8**.

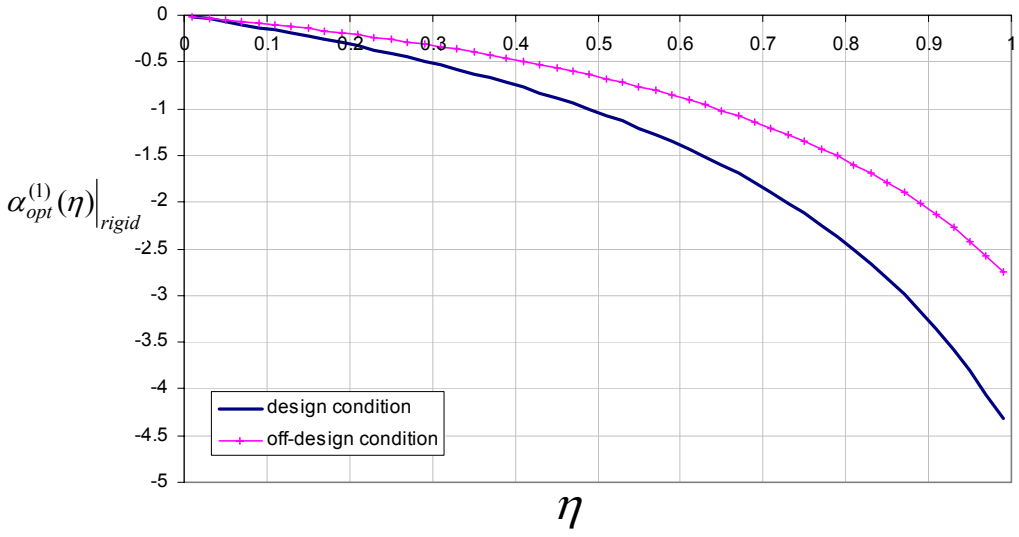


**Figure** 12**: SLW Type: Rigid wing optimal geometric twist distribution for design and off-design flight conditions,** $\alpha_{opt}^{(1)}(\eta)\big|_{rigid}$ **(**$\overline{\alpha}_{opt}^{(1)} = 7.07^\circ$**) and** $\alpha_{opt}^{(2)}(\eta)\big|_{rigid}$ **(**$\overline{\alpha}_{opt}^{(2)} = 4.89^\circ$**)**

*Step2 :*

Next, we found the angle of attack $\overline{\alpha}^{(2)}$ that generates the off-design condition $C_L^{(2)} = 0.42$ when we use the geometric twist of design condition, $\alpha_{opt}^{(1)}(\eta)\big|_{rigid}$ as shown in the last column of the **Table 8**. Comparing the last two columns of **Table 8**, the design condition optimal geometric twist and the adjusted angle of attack for the off-design condition resulted in a lower span efficiency factor than the off-design optimal twist and angle of attack, $e_{\max}^{(2)} > e^{(2)}$. There is about a 0.6 drag count increase that corresponds to a 0.8% reduction in span efficiency when the structural deformation is included in the analysis.

**Table** 8**: Rigid wing analyses for SLW Type distribution** $\alpha_{tot}(\eta)$**: Effect of constant angle of attack adjustment on drag optimum swept-tapered wing for** $C_L^{(1)} = 0.6$**.**

| | Design condition (1) Optimal wing | Off-design condition (2) Optimal wing | Off-design condition (2) Non-optimal wing |
|---|---|---|---|
| Lift coefficient, $C_L$ | $C_L^{(1)} = 0.6$ | $C_L^{(2)} = 0.42$ | $C_L^{(2)} = 0.42$ |
| Geometric twist, $\alpha(\theta)$ | $\alpha_{opt}^{(1)}(\eta)\big\|_{rigid}$ | $\alpha_{opt}^{(2)}(\eta)\big\|_{rigid}$ | $\alpha_{opt}^{(1)}(\eta)\big\|_{rigid}$ |
| Angle of attack, $\overline{\alpha}$ | $\overline{\alpha}_{opt}^{(1)} = 7.07^o$ | $\overline{\alpha}_{opt}^{(2)} = 4.89^o$ | $\overline{\alpha}^{(2)} = 5.22^o$ |
| Span efficiency, $e$ | $e_{\max}^{(1)} = 0.99722$ | $e_{\max}^{(2)} = 0.99755$ | $e^{(2)} = 0.98937$ |
| Induced drag coefficient, $C_{D_i}$ | 0.015321 | 0.007505 | 0.007567 |
| Induced drag penalty | | $\dfrac{e_{\max}^{(2)} - e^{(2)}}{e_{\max}^{(2)}} = 0.008$ | |

*Step 3:*

The lift coefficient of the off-design conditions as a function of the angle of attack, are shown in **Figure** 13 and **Figure** 14, respectively for the Scenario I and Scenario II.

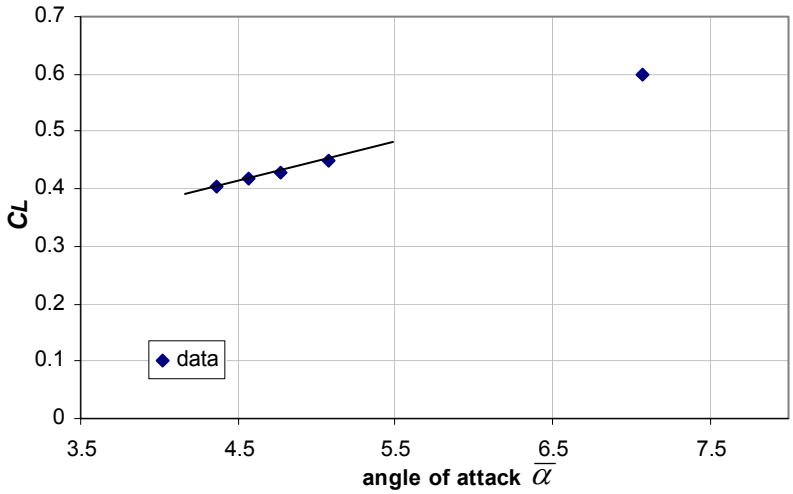


**Figure** 13**: Twist B, Scenario I: The lift coefficient versus angle of attack after step 3**

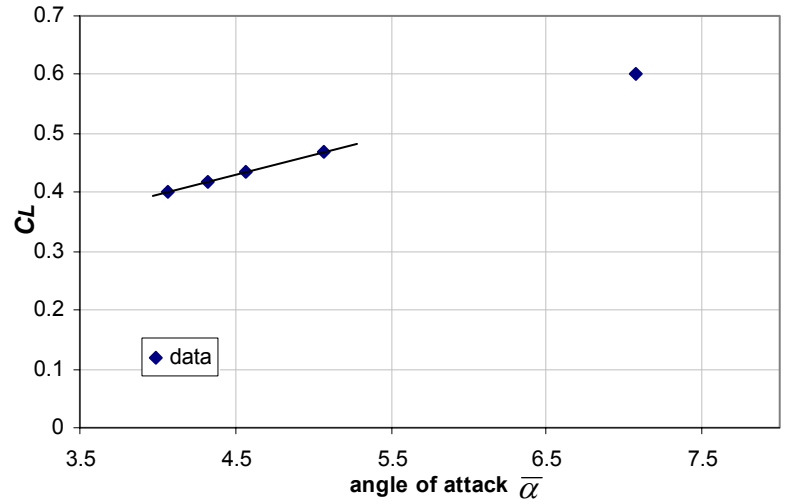


**Figure** 14**: Twist B, Scenario II: The lift coefficient versus angle of attack after step 3**

*Step 4:*

From the data generated in step 3 the angle of attack for Scenario I was determined as $\overline{\alpha}^{(2)}\Big|_{I} = 4.62^{\circ}$ and for scenario II as $\overline{\alpha}^{(2)}\Big|_{II} = 4.36^{\circ}$, both associated with the target off-design lift coefficient of $C_L^{(2)}$=0.42. Recall that $\alpha_{tot}^{(2)}(\eta) = \alpha_{tot}(\eta)\Big|_{\overline{\alpha}^{(2)}}$, so the total angle of incidence distributions for the optimal case, scenario I and scenario II of the off-design condition can now be shown in **Figure** 15. Spanloads associated with the off-design condition optimal wing and two non-optimal settings based on the optimal design condition wing (Scenario I and II) are shown in **Figure** 16 for the SLW Type twist distribution, straight-line wrapped surfaces. The deviation from the optimal spanload does not seem to be as significant as it was reflected in the induced drag penalty results.

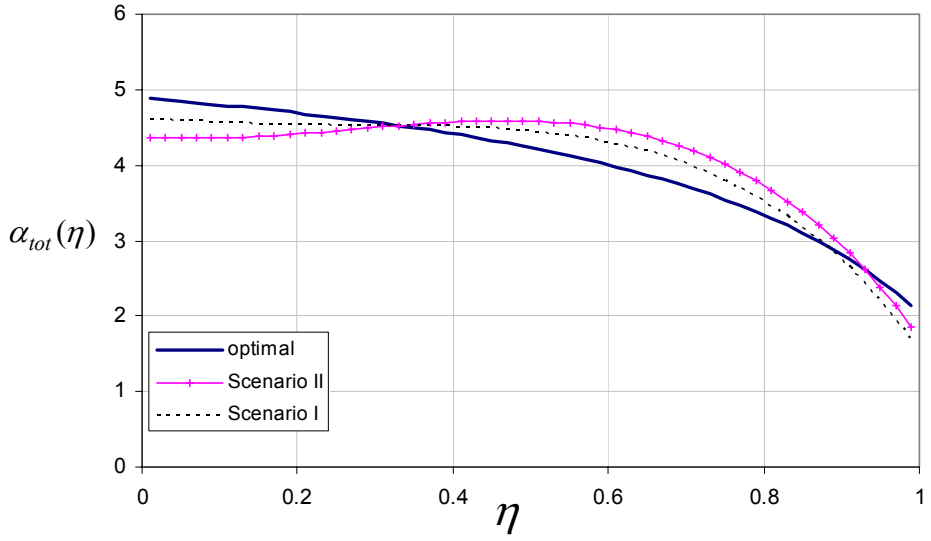


**Figure** 15**: SLW Type, comparison of total angle of incidence, $\alpha_{tot}(\eta)$ : Optimal wing for off-design condition versus the non-optimal wings**

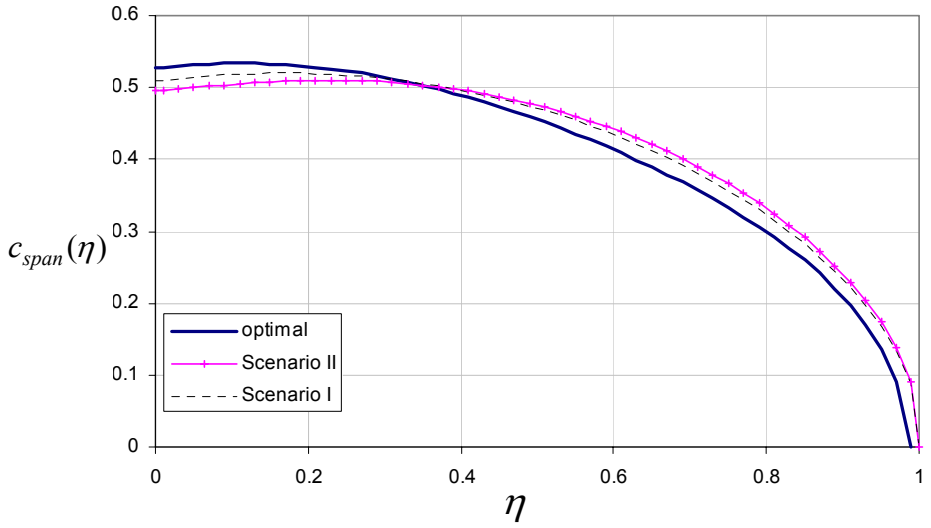


**Figure** 16**: SLW Type, spanload comparison, $c_{span}(\eta)$ : Optimal wing for off-design condition versus the non-optimal wings**

Finally **Table 9** was prepared to summarize the results for the induced drag penalty of the SLW Type twist. The second and third columns of **Table 9** present the optimal wings at the design and off-design flight conditions under the constraint of straight line wrapped surfaces, respectively. The induced drag penalty can be determined by comparing column three (the wing tailored for the off-design conditions) with the last two columns (the non-optimal wing based on the optimal wing of the design flight condition and the angle of attack adjustment). The reduction in the span efficiency factor is less than 0.5%. This corresponds to an increase in the induced drag of less than one drag-count.

Note that the span efficiency factors reported in the second and third columns of **Table 6** are higher than those of **Table 9**. The induced drag penalty for the SLW Type twist, however, is lower than that of ED Type twist. In other

words, although the twist for an elliptic spanload is more effective than the twist of a straight line wrapped surface, the latter seemed to be less sensitive to changes due to structural deformation and may be preferred if tailoring the structure for the off-design conditions is not an option.

**Table 9: Effect of constant angle of attack adjustment on drag optimum swept-tapered wing of Twist B for** $C_L^{(1)} = 0.6$ .

| | Design (1) Optimal wing | Off-design (2) Optimal wing | Off-design (2) Non-optimal wing Scenario I | Off-design (2) Non-optimal wing Scenario II |
|---|---|---|---|---|
| Lift coefficient, $C_L$ | $C_L^{(1)} = 0.60$ | $C_L^{(2)} = 0.42$ | $C_L^{(2)} = 0.42$ | $C_L^{(2)} = 0.42$ |
| Total angle of incidence, $\alpha_{tot}(\eta)$ | $\alpha_{tot}^{(1)}(\eta)\big\|_{opt}$ | $\alpha_{tot}^{(2)}(\eta)\big\|_{opt}$ | $\alpha_{tot}^{(2)}(\eta) = \alpha_{tot}(\eta)\big\|_{\bar{\alpha}^{(2)}}$ | $\alpha_{tot}^{(2)}(\eta) = \alpha_{tot}(\eta)\big\|_{\bar{\alpha}^{(2)}}$ |
| Angle of attack, $\bar{\alpha}$ | $\bar{\alpha}_{opt}^{(1)} = 7.07^{o}$ | $\bar{\alpha}_{opt}^{(2)} = 4.89^{o}$ | $\bar{\alpha}^{(2)}\big\|_{I} = 4.62^{\circ}$ | $\bar{\alpha}^{(2)}\big\|_{II} = 4.36^{\circ}$ |
| Span efficiency, $e$ | $e_{\max}^{(1)} = 0.99722$ | $e_{\max}^{(2)} = 0.99755$ | $e^{(2)} = 0.99728$ | $e^{(2)} = 0.99359$ |
| Induced drag coefficient, $C_{D_i}$ | 0.015321 | 0.00750 | 0.00751 | 0.00757 |
| Induced drag penalty, $\frac{e_{\max}^{(2)} - e^{(2)}}{e_{\max}^{(2)}}$ | | | 0.0003 | 0.004 |

## V. CONCLUDING REMARKS

The optimal wing for a particular flight condition was studied at off-design flight conditions. The metric of interest was the span efficiency factor allowing us to evaluate the induced drag penalty that may be caused by the changes in the spanload and the total angle of incidence as the flight condition changes. Two types of total angle of incidence distributions for design flight conditions were investigated while considering the off-design condition as the flight at a lower lift coefficient than the lift coefficient associated with the design flight condition. For both distribution types we demonstrated how changes in the flight condition and static aeroelastic response affect the angle of incidence distribution and the spanload. For the distribution offering near elliptic spanload (near optimal wing with respect to induced drag) such changes resulted in about a two drag-count increase which may be sufficient to suggest tailoring the structure as the flight condition changes. The second type was the total angle of incidence distribution associated with the straight-line wrapped surfaces for which the span efficiency at the design condition was lower due to the constraint on the distribution that results in non-elliptic spanload. It was found, however, more effective at the off-design conditions if the wing was not tailored because it was insensitive to the structural deformation and the penalty level was lower.

## REFERENCES


[1.] Lynch, R. W. and Rogers, W. A. (1976), "Aeroelastic Tailoring of Composite Materials to Improve Performance," Proceedings of AIAA/ASME/SAE, 17th Structures, Structural Dynamics, and Materials Conference, King of Prussia, PA.

[2.] Haftka, R. T. (1977), "Optimization of Flexible Wing Structures Subject to Strength and Induced Drag Constraints," AIAA Journal, 15 (8), pp. 1101-1106.

[3.] Anderson, J. D., Jr., (1985), Fundamentals of Aerodynamics, McGraw-Hill.

[4.] Rasmussen, M. L. and Smith, D. E., (1999), "Lifting-Line Theory for Arbitrarily Shaped Wings," Journal of Aircraft. 36 (2), p 340-348.

[5.] Lamar, J. E., (1976), "A Vortex Lattice Method for the Mean Camber Shapes of Trimmed Non-Coplanar Planforms with Minimum vortex Drag," NASA TN D-8090.

[6.] Craig, A. P. and McLean J. D. (1988), "Spanload Optimization for Strength Designed Lifting Surfaces," AIAA 6th Applied Aerodynamics Conference, Williamsburg, VA.

[7.] Iglesias, S. and Mason, W. H., "Optimum Spanloads Incorporating Wing Structural Weight," 1st AIAA Aircraft Technology, Integration, and Operations Forum, 16-18 October 2001, Los Angeles, CA, AIAA-2001-5234.

[8.] Gern, F. H., Naghshineh-Pour, A. H., Sulaeman, E., Kapania, R. K. and Haftka, R. T., (2001), "Structural Wing Sizing for Multidisciplinary Design Optimization of a Strut-Braced Wing," Journal of Aircraft, 38 (1), pp. 154-163.

[9.] Gern, F. H., Inman, D. J. and Kapania, R. K., (2002), "Structural and Aeroelastic Modeling of General Planform Wings with Morphing Airfoils," AIAA Journal, 40 (4), pp. 628-637.

[10.] MSC.NASTRAN Version 68 (2002) Aeroelastic Analysis Users's Guide, MSC Software Corporation, 2 MacArthur Place, Santa Ana, CA, 92707.

[11.] http://www.aoe.vt.edu/~mason/Mason_f/MRsoft.html#lidrag.

[12.] Digital Dutch, 1976 Standard Atmosphere Calculator, last accessed on 11/10/2003, http://www.digitaldutch.com/atmoscalc/.


## APPENDIX A: POTENTIAL DRAG PENALTY DUE TO OPTIMAL TWIST CHANGING WITH FLIGHT CONDITION

Consider a rigid wing of any planform with a spanwise geometric twist distribution $\alpha(\theta)$ (after making the transformation for spanwise coordinate, *y*, of the wing of span $b$ as $y = \frac{b}{2}\cos\theta$ with $\theta \in [0, \pi]$). Suppose that the wing has an elliptical circulation (lift) and minimum induced drag at two different angles of attack, $\overline{\alpha}^{(1)}$ and $\overline{\alpha}^{(2)}$ corresponding to two different lift coefficients $C_L^{(1)}$ and $C_L^{(2)}$, respectively. That is, the spanwise total angle of incidences $\alpha(\theta) + \overline{\alpha}^{(1)}$ and $\alpha(\theta) + \overline{\alpha}^{(2)}$ provide elliptical $\Gamma^{(1)}(\theta)$ and $\Gamma^{(2)}(\theta)$ as

$$\Gamma^{(1)}(\theta) = A^{(1)} \sin\theta, \tag{14}$$

$$\Gamma^{(2)}(\theta) = A^{(2)} \sin\theta. \tag{15}$$

Note that the difference of the two circulations is also elliptical and should correspond to the wing of the same planform with no twist, but at an angle of attack, $\Delta\overline{\alpha} = \overline{\alpha}^{(1)} - \overline{\alpha}^{(2)}$. Constant angle of incidence, $\Delta\overline{\alpha}$ along the span (no twist) and elliptical circulation is only possible if the wing also has an elliptic chord distribution (Anderson, 1985). This specific requirement regarding the planform states that the wing of a general planform may achieve minimum induced drag (elliptical circulation) at different lift coefficients $C_L$ (different flight conditions) only if the twist distribution is tailored for the levels of $C_L$ (flight conditions). A more formal (analytical) evaluation regarding the drag penalty potential as the flight condition changes using the Prandtl's lifting line theory (Appendix B) may be found in Appendix C.

## APPENDIX B: PRANDTL'S LIFTING LINE THEORY (DUE TO RASMUSSEN AND SMITH 1999)

The geometric angle of attack (twist) for a finite wing can be expressed via Prantdl's lifting line theory (Anderson, 1984 and Rasmussen and Smith, 1999),

$$\alpha(\theta) = \frac{2\Gamma(\theta)}{V_\infty m_0(\theta) c(\theta)} + \alpha_{L=0}(\theta) + \alpha_i(\theta)\,, \tag{16}$$

where $\Gamma(\theta)$ is the spanwise circulation distribution (after making the transformation $y = \frac{b}{2}\cos\theta$ with $\theta \in [0, \pi]$). $\alpha_{L=0}(\theta)$ is the zero lift angle of attack of the airfoil, $m_0(\theta)$ is the airfoil lift curve slope (can be taken as $2\pi$ based on thin airfoil assumption). The wing chord distribution along the span is denoted by $c(\theta)$. Last term $\alpha_i(\theta)$ in Eq. (16) is induced angle of attack due to the downwash velocity for the finite wing and can be written as,

$$\alpha_i(\theta) = \frac{1}{2\pi b V_\infty} \int_0^\pi \frac{(d\Gamma / d\bar{\theta})}{\cos\bar{\theta} - \cos\theta} d\bar{\theta} \tag{17}$$

The lift coefficient for the local airfoil at $\theta \in [0, \pi]$ are given as

$$c_l(\theta) = m_0(\theta)\left[\alpha_a(\theta) - \alpha_i(\theta)\right] \tag{18}$$

where $\alpha_a(\theta)$ is the absolute angle of attack obtained by the difference between geometric and aerodynamic twists,

$$\alpha_a(\theta) = \alpha(\theta) - \alpha_{L=0}(\theta) \tag{19}$$

The local lift coefficient can also be expressed in terms of circulation and chord distributions,

$$c_l(\theta) = \frac{2\Gamma(\theta)}{V_\infty c(\theta)} \tag{20}$$

The resultant lift and induced drag coefficients are

$$C_L = \frac{L}{q_\infty S} = \frac{b}{V_\infty S} \int_0^\pi \Gamma(\theta) \sin\theta d\theta \tag{21}$$

$$C_{D_i} = \frac{D_i}{q_\infty S} = \frac{b}{V_\infty S} \int_0^\pi \Gamma(\theta)\alpha_i(\theta) \sin\theta d\theta \tag{22}$$

where *S* is the wing area. We can write the general circulation distribution and the straight wing chord as a Fourier sine series of odd terms by taking the symmetry into account (Rasmussen and Smith, 1999),

$$\Gamma(\theta) = \frac{1}{2} m_{0r} c_r V_\infty \sum_{n=0}^{\infty} A_{2n+1} \sin(2n+1)\theta\,, \tag{23}$$

$$c(\theta) = c_r \sum_{n=0}^{\infty} C_{2n+1} \sin(2n+1)\theta\,, \tag{24}$$

where $m_{0r}$ and $c_r$ are the root airfoil lift curve slope ( $m_0$ at *y*=0, i.e. $\theta = \pi/2$ ) and root chord, respectively. The coefficients in Eq. (24) can be found via,

$$C_{2n+1} = \frac{4}{\pi} \int_0^{\pi/2} \frac{c(\theta)}{c_r} \sin(2n+1)\theta d\theta \tag{25}$$

and the wing area is,

$$S = \frac{b}{2} \int_0^\pi c(\theta) \sin\theta d\theta = \frac{\pi b c_r}{4} C_1 \tag{26}$$

Spanwise distribution of the absolute angle of attack can also be represented as a Fourier cosine series (even terms only due to symmetry),

$$\alpha_a(\theta) = \sum_{n=0}^{\infty} a_{2n} \cos 2n\theta\,, \tag{27}$$

and the coefficients are

$$a_0 = \frac{2}{\pi}\int_0^{\pi/2} \alpha_a(\theta)d\theta$$
$$a_{2n} = \frac{4}{\pi}\int_0^{\pi/2} \alpha_a(\theta)\cos 2n\theta d\theta, \qquad n = 1,2,\ldots \tag{28}$$

Substituting Eq. (23) in Eq. (17), induced angle of attack can now be rewritten as,

$$\alpha_i(\theta) = \frac{m_{or}c_r}{4}\sum_{n=0}^{\infty}(2n+1)A_{2n+1}\frac{\sin(2n+1)\theta}{\sin\theta} \tag{29}$$

Rasmussen and Smith (1999) also used the following alternative series form in order to simplify the further complications due to singularity in Eq. (29),

$$\alpha_i(\theta) = \frac{m_{0r}c_r}{4b}\sum_{n=0}^{\infty}B_{2n}\cos 2n\theta \tag{30}$$

where

$$B_0 = \sum_{m=0}^{\infty}(2m+1)A_{2m+1}$$
$$B_{2n} = 2\sum_{m=n}^{\infty}(2m+1)A_{2m+1} \qquad n = 1,2,3\ldots \tag{31}$$

Following Rasmussen and Smith (1999), we can write the lifting line equation as ( $m_{0r} = m_0$ ),

$$\frac{1}{2}\left\{a_0 C_{2n+1} + \sum_{k=0}^{\infty}\left[a_{|n-k|} - a_{2(n+k+1)}\right]C_{2k+1}\right\}$$
$$-\frac{1}{2}\frac{m_0}{\pi ARC_1}\left\{B_0 C_{2n+1} + \sum_{k=0}^{\infty}\left[B_{2|n-k|} - B_{2(n+k+1)}\right]C_{2k+1}\right\} = A_{2n+1} \quad n = 0,1,2\ldots \tag{32}$$

Equation (32) results in a system of equations to determine directly the spanload, i.e., circulation distribution once the wing geometry including chord and twist distributions are known (alternatively solved by collocation method). Rasmussen and Smith (1999) reported the system of equations as the following for solving the coefficients $A_{2n+1}$,

$$\sum_{n=0}^{\infty}C_{(2m+1),(2n+1)}A_{2n+1} = D_{2m+1,} \qquad m = 0,1,2,\ldots \tag{33}$$

where

$$C_{(2m+1),(2n+1)} = \delta_{(2m+1)(2n+1)} + \frac{(2n+1)m_0}{\pi ARC_1}\sum_{k=|m-n|}^{m+n}C_{2k+1,} \qquad m,n = 0,1,2,\ldots \tag{34}$$

and

$$D_{2n+1} = \frac{1}{2}\left\{a_0 C_{2n+1} + \sum_{k=0}^{\infty}\left[a_{2|n-k|} - a_{2(n+k+1)}\right]C_{2k+1}\right\}, \qquad m,n = 0,1,2,\ldots \tag{35}$$

Then the lift and induced drag characteristics of the given wing and determined spanload can be evaluated by the total lift and induced drag coefficients,

$$C_L = \frac{b\pi m_{or}c_r}{4S}A_1 = \frac{m_{or}}{C_1}A_1 \tag{36}$$

$$C_{D_i} = \frac{C_L^2}{\pi b^2/S}(1+\delta) \tag{37}$$

where

$$\delta = \sum_{n=1}^{\infty}(2n+1)\left(\frac{A_{2n+1}}{A_1}\right)^2. \tag{38}$$

## APPENDIX C: ANALYTICAL EVALUATION OF POTENTIAL DRAG PENALTY AS THE FLIGHT CONDITION CHANGES

Minimum induced drag occurs when $\delta$ =0 ($e$=1), and that corresponds to elliptic circulation and lift distribution. Therefore we can consider $\delta$ as the induced drag penalty relative to an elliptic circulation distribution.

For a rigid wing with no structural deformation, we consider two cruise flight conditions of the same cruise speed and weight, but at different altitudes. That is, two lift requirements for the same wing; $C_L^{(1)}$ and $C_L^{(2)}$ corresponding to the two altitudes. The two cases will require two separate geometric twist distributions $\alpha^{(1)}(\theta)$ and $\alpha^{(2)}(\theta)$ to achieve elliptical circulation (lift) and minimum induced drag associated with the cruise conditions.

The resultant elliptic circulation distributions can be expressed by assigning coefficients of Fourier sine series as zero except the first coefficient ( $A_{2n+1} = 0$ for $n \neq 0$ )

$$\Gamma^{(1)}(\theta) = \frac{1}{2} m_{or} c_r V_\infty A_1^{(1)} \sin\theta \,, \tag{39}$$

$$\Gamma^{(2)}(\theta) = \frac{1}{2} m_{or} c_r V_\infty A_1^{(2)} \sin\theta \,. \tag{40}$$

where $m_{or}$ and $c_r$ are the lift curve slope and the chord length at the root, respectively, and $V_\infty$ is the freestream velocity. For $C_L^{(2)} = rC_L^{(1)}$ (see Eq. (57)), the first coefficient of the series is found to be $A_1^{(2)} = rA_1^{(1)}$, so that induced angles of attack for the two cases are related as,

$$\alpha_i^{(2)}(\theta) = r\alpha_i^{(1)}(\theta) \,. \tag{41}$$

Substituting Eqs. (39)-(41) into classical lifting line equation we can express the geometric angle of attack (geometric twist) associated with the two cases of minimum induced drag,

$$\alpha^{(1)}(\theta) = \frac{2\Gamma^{(1)}(\theta)}{V_\infty m_0(\theta) c(\theta)} + \alpha_{L=0}(\theta) + \alpha_i^{(1)}(\theta) \,, \tag{42}$$

$$\alpha^{(2)}(\theta) = \frac{2r\Gamma^{(1)}(\theta)}{V_\infty m_0(\theta) c(\theta)} + \alpha_{L=0}(\theta) + r\alpha_i^{(1)}(\theta) \,. \tag{43}$$

Consider now the rigid wing providing minimum induced drag at cruise altitude corresponding to $C_L^{(1)}$ and the optimal twist $\alpha^{(1)}(\theta)$. For this design also to have minimum induced drag at the other cruise altitudes for the same cruise weight and speed, one should be able to achieve geometric angle of attack $\alpha^{(2)}(\theta)$, for instance, by a constant adjustment in the angle of attack, $\overline{\alpha}$, that is,

$$\alpha^{(2)}(\theta) = \alpha^{(1)}(\theta) + \overline{\alpha} \,, \tag{44}$$

Note that the angle of attack adjustment $\overline{\alpha}$ is negative if the ratio $r$ is less than unity, and positive if the ratio $r$ is more than unity. Equations (42)-(44), however, result in a contradiction as the adjustment in angle of attack $\overline{\alpha}$ should vary spanwise, in general:

$$\overline{\alpha} = (r-1)\left[\alpha^{(1)}(\theta) - \alpha_{L=0}(\theta)\right], \tag{45}$$

Constant $\overline{\alpha}$ along the span is only possible if the wing also has an elliptic chord distribution, no geometric and aerodynamic twist, i.e. $\alpha^{(1)}$ and $\alpha_{L=0}$ are constant along the span (Anderson, 1985).

## APPENDIX D: INDUCED DRAG PENALTY AS CRUISE ALTITUDE CHANGES USING LLT FOR RIGID STRAIGHT WINGS

The geometric angle of attack (geometric twist) for a finite straight wing (no sweep) can be expressed via Prantdl's lifting line theory (Anderson, 1984 and Rasmussen and Smith, 1999),

$$\alpha(\theta) = \frac{2\Gamma(\theta)}{V_\infty m_0(\theta) c(\theta)} + \alpha_{L=0}(\theta) + \alpha_i(\theta)\,, \tag{46}$$

where $\Gamma(\theta)$ and $c(\theta)$ are the spanwise circulation and chord distributions, respectively. Also, $\alpha_{L=0}(\theta)$ and $m_0(\theta)$ are the zero lift angle of attack of the airfoil (aerodynamic twist) and the airfoil lift curve slope along the span, respectively.

The induced drag coefficient for a given lift coefficient $C_L$ is expressed as,

$$C_{D_i} = \frac{C_L^2}{e\pi AR}\,. \tag{47}$$

where span efficiency factor $e = (1+\delta)^{-1}$, and $\delta$ can be written as a function of Fourier sine series coefficients $A_{2n+1}$ representing the circulation (see Appendix B),

$$\delta = \sum_{n=1}^{\infty} (2n+1)\left(\frac{A_{2n+1}}{A_1}\right)^2\,. \tag{48}$$

Minimum induced drag occurs when $\delta$ =0 ($e$=1), and that corresponds to elliptic circulation and lift distribution. Therefore we can consider $\delta$ as the induced drag penalty relative to an elliptic circulation distribution.

For a rigid wing with no structural deformation, we consider two cruise flight conditions of the same cruise speed and weight, but at different altitudes. That is, two lift requirements for the same wing; $C_L^{(1)}$ and $C_L^{(2)}$ corresponding to the two altitudes. The two cases will require two separate geometric twist distributions $\alpha^{(1)}(\theta)$ and $\alpha^{(2)}(\theta)$ to achieve elliptical circulation (lift) and minimum induced drag associated with the cruise conditions.

For a straight wing of taper ratio $\lambda$, the chord along the semispan can be expressed as

$$c(\theta) = c_r\left[1-(1-\lambda)\cos\theta\right], \tag{49}$$

where $c_r$ is the chord length at the root. Assume that the lift curve slope is constant along the span $m_0$ and the geometric twist $\alpha^{(1)}(\theta)$ for the wing is such that the elliptic spanload is achieved for $C_L^{(1)}$,

$$\Gamma^{(1)}(\theta) = \frac{1}{2} m_{or} c_r V_\infty A_1^{(1)} \sin\theta\,, \tag{50}$$

where $m_{or}$ is the lift curve slope at the root and $V_\infty$ is the freestream velocity. The absolute angle of attack is the difference between geometric and aerodynamic angles of attack or twists $\alpha(\theta)$ and $\alpha_{L=0}(\theta)$, respectively, and for such an induced drag optimum wing it is given as,

$$\alpha_a^{(1)} = A_1^{(1)}\left\{\frac{\sin\theta}{1-(1-\lambda)\left|\cos(\theta)\right|} + \frac{m_0}{\pi AR C_1}\right\}, \tag{51}$$

where $C_1$ is a constant as a function of the chord distribution [Eq. (25) in the appendix A]. If the absolute angle of attack is expressed as a Fourier cosine series, associated constants $a_{2n}$ can be found as [see appendix A, Eq. (28)]

$$\begin{aligned} a_0^{(1)} &= A_1^{(1)}\,\frac{2}{\pi}\left[\frac{\ln(\lambda)}{\lambda-1} + \frac{m_0}{2AR C_1}\right] \\ a_{2n}^{(1)} &= A_1^{(1)}\,\frac{4}{\pi}\left[\frac{\ln(\lambda)}{\lambda-1} + \frac{2n}{(1-\lambda)}\int_0^{\pi/2} \ln\left[1-(1-\lambda)\cos\theta\right]\sin 2n\theta\, d\theta\right], \quad n = 1,2,3,\ldots \end{aligned}\,, \tag{52}$$

Now we like to find the spanload of the same wing, same cruise speed and weight, but for a different cruise altitude, and $C_L^{(2)} = rC_L^{(1)}$. The absolute angle of attack is now

$$\alpha_a^{(2)} = \alpha_a^{(1)} + \overline{\alpha} \,. \tag{53}$$

where $\overline{\alpha}$ is the adjustment in the angle of attack that is to be determined for a given factor $r$ (note that $\overline{\alpha}$ is negative if the ratio $r$ is less than unity, and positive if the ratio $r$ is more than unity). This will give the coefficients as

$$\begin{aligned} a_0^{(2)} &= a_0^{(1)} + \overline{\alpha} \\ a_{2n}^{(2)} &= a_{2n}^{(1)}, \quad n = 1,2,3,\ldots \end{aligned}, \tag{54}$$

We know that $A_1^{(2)} = rA_1^{(1)}$ (see the appendix A), but need to determine the rest of the coefficients of the circulation function ( $A_{2n+1}^{(2)}$ for $n = 1,2,\ldots$ ). If we modify the system of equations in Eq. (32) of the appendix A for solving $A_{2n+1}^{(2)}$ ( $n = 1,2,3,\ldots$ ) and $\overline{\alpha}$ by substituting $A_1^{(2)} = rA_1^{(1)}$ and Eq. (54), we obtain

$$\sum_{n=1}^{\infty} C_{(2m+1),(2n+1)} A_{2n+1}^{(2)} - C_{2m+1}\overline{\alpha} = D_{2m+1}^{(1)} - rC_{(2m+1),1} A_1^{(1)} \qquad m = 0,1,2,\ldots \tag{55}$$

**A. Rectangular wing**

For simplicity, consider first the wing to be rectangular shape ( $\lambda = 1$ ) for which the integral in Eq. (52) can be solved analytically, and the coefficients are

$$\begin{aligned} a_0^{(1)} &= A_1^{(1)} \left[ \frac{2}{\pi} + \frac{m_0}{\pi AR C_1} \right] \\ a_{2n}^{(1)} &= A_1^{(1)} \frac{4}{\pi} \frac{1}{1-4n^2}, \quad n = 1,2,3,\ldots \end{aligned}, \tag{56}$$

We can solve Eq. (55) for a given lift ratio $r$, and substitute the coefficients $A_{2n+1}^{(2)}$ into Eq. (48) for the drag penalty. **Figure 17** summarizes the drag penalty results, $\delta * 100$ as a function of the lift ratio $r$ (between 0 and 1) for the rectangular wing. As the ratio decreases the penalty relative to its optimum case (elliptic distribution at $r$) increases.

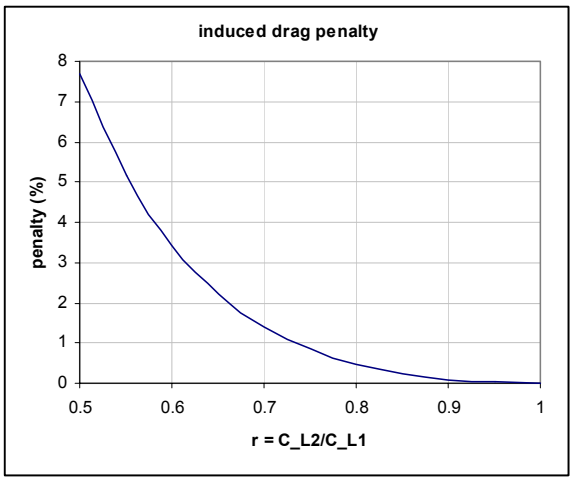


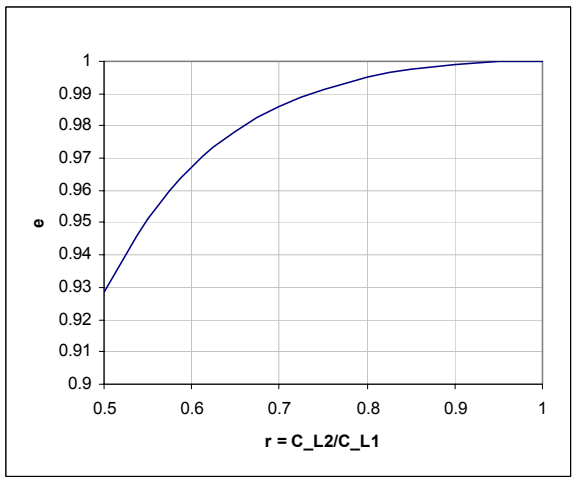


**Figure 17: Induced drag penalty when the cruise weight is different than the design weight for which the associated induced drag is minimum.** $AR$**=9,** $\lambda = 1$**,** $m_0 = 2\pi$ **.**

**B. Unswept-tapered wing**

It is also important to check how this penalty may be affected by the taper ratio as it helps to achieve the elliptical distribution. The integral in Eq. (52) is solved numerically and induced drag penalty is computed for $r = 0.7$ as the taper ratio changes. The least drag penalty happens when the taper ratio is about $\lambda = 0.35$ . **Figure**

**18** shows how the taper ratio improves on the drag penalty. **Figure 19** shows the circulation elliptic distribution associated with the altitude of $C_L^{(1)}$, the circulation associated with the altitude of $C_L^{(2)}$ when the wing is designed for altitude of $C_L^{(1)}$, and the elliptic circulation distribution associated with the altitude of $C_L^{(2)}$. Distributions for flight condition (2) are very close which results drag penalty of less than 1%.

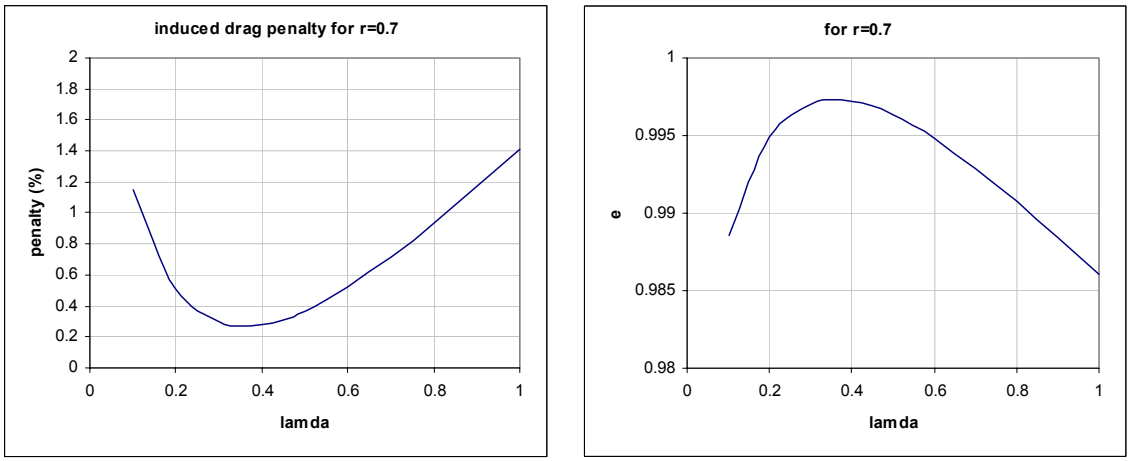


**Figure** 18**: Taper ratio effect on the induced drag penalty.:***AR*=**9,** $r = 0.7$**,** $m_0 = 2\pi$ **.**

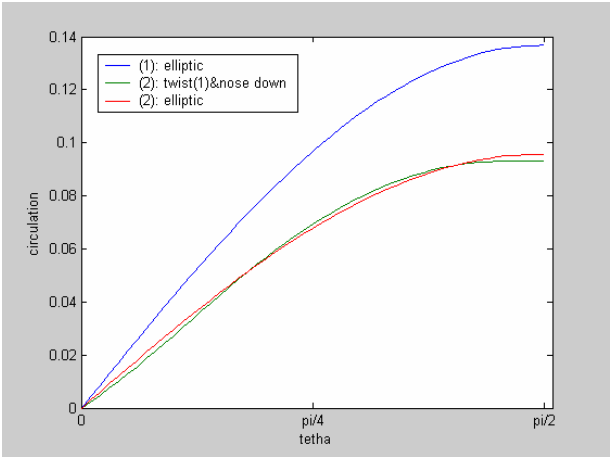


**Figure** 19**: Circulation distributions for taper ratio 0.35 (***AR*=**9,** $r = 0.7$**,** $m_0 = 2\pi$ **)**

## APPENDIX E: EFFECT OF ALTITUDE ON LIFT COEFFICIENT

The effect of different altitudes may simply be assessed by the change in air density and the speed of sound. For a given Mach number and cruise weight the cruise altitude determines the flight lift coefficient $C_L$. The air density and speed of sound at the optimum altitude are denoted as $\rho^{(1)}$ and $a^{(1)}$, respectively, and that yields to lift coefficient $C_L^{(1)}$. The air density $\rho^{(2)}$ and speed of sound $a^{(2)}$ at a different altitude result in a different lift coefficient $C_L^{(2)}$ and Eq. (57) relates the lift coefficients as,

$$r = \frac{C_L^{(2)}}{C_L^{(1)}} = \frac{\rho^{(1)}}{\rho^{(2)}} \left( \frac{a^{(1)}}{a^{(2)}} \right)^2 . \tag{57}$$

**Figure** 20 shows how the ratios of the air density (Digital Dutch 2003) and the lift coefficient (Eq. (57)) change with the altitude relative to a reference or design altitude of about 13km (~43000 ft). The ratio *r* is influenced even more as in the case of shorter hops with lower cruise weight due to less fuel on board and possibly less payload.

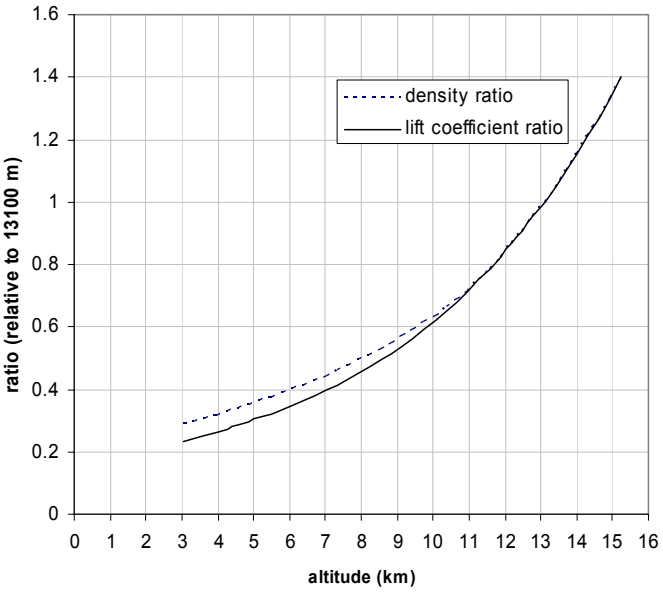


**Figure** 20**: Variation of the air density and lift coefficient with the altitude - normalized by figures at an altitude of 13100 m (43000 ft) (data due to Digital Dutch 2003**